Depositional setting and U-Pb detrital record of rift-related deposits in the Moeda Formation (Minas Supergroup) at the Gandarela and Ouro Fino synclines, Quadrilátero Ferrífero, Brazil

Rafael da Silva Madureira[1,2]* ⓘ, Maximiliano Martins[1] ⓘ, Gláucia Queiroga[1] ⓘ, Cristiano Lana[1] ⓘ, Luiz Fernandes Dutra[3] ⓘ, Ana Ramalho Alkmim[1] ⓘ

Abstract

The Moeda Formation (Caraça Group, base of Minas Supergroup) registers the initial rift stages of the Minas Basin in the Quadrilátero Ferrífero, Southern São Francisco craton, SE-Brazil. We present stratigraphic and U-Pb detrital zircon dating analyses of the Moeda Formation that contribute to the comprehension of its sedimentary evolution in the southernmost Gandarela and Ouro Fino synclines (Central-Eastern Quadrilátero Ferrifero). The Moeda Formation sequence consists of a basal proximal alluvial fan with clast-supported conglomerates, grading upward into an alluvial floodplain with quartz arenites, and upper massive sandstones from distal fluvial fans. Because the Moeda Formation is normally limited by similar lithologies at both its base (Nova Lima Group, Rio das Velhas Supergroup) and top (Batatal Formation, uppermost Caraça Group) and stratigraphic inversion has occurred in the study area, U-Pb detrital zircon dating was also extended to these units to differentiate them stratigraphically. The youngest clusters of detrital zircon ages in the Nova Lima Group and Moeda and Batatal formations were 2716, 2777 and 2786 Ma, respectively. Based on our data and relevant literature, the depositional age of the Moeda Formation was interpreted as between 2716 and 2520 Ma with the Mesoarchean continental crust, the Rio das Velhas Supergroup and the Archean TTG complexes as its main source areas.

KEYWORDS: high-resolution stratigraphic framework; facies analysis; zircon U-Pb geochronology; Minas Basin; Moeda Formation.

INTRODUCTION

Embryonic stages of continental rifting are characterized by the formation of small wedge-shaped depocenters bounded by isolated normal faults segments (Lewis *et al.* 2015), representing the first tectonic steps, which precedes the development of overall drift phases (Condie 2014).

The deposition of syn-rift units reflects ongoing fault activity that controls the uplifting of the basement blocks and the basin fill architecture, as well as its depositional environments (Lewis *et al.* 2015). There is a special meaning for those Proterozoic analogs, in which provenance studies have been successfully used as important tools to support paleoenvironmental and paleotectonic reconstructions (Einsele 2000, Miall 2000).

The Moeda Formation (Wallace 1958, Dorr II 1969) records the rifting event that reached the Southern São Francisco paleoplate on the Archean-Paleoproterozoic boundary (Dopico *et al.* 2017). It is the lowermost unit of the Minas Supergroup (MS) in the Quadrilátero Ferrífero (QF) mining district and is related to a continental rift basin followed by a passive margin phase (Alkmim and Marshak 1998).

The Moeda Formation's syn-rift deposits were recognized in the northern QF, initially at the Moeda and Gandarela plateaus (Lindsey 1975, Villaça 1981), and later in the Caraça range (Rosseto *et al.* 1987). They mark the rifting zone of the Moeda basin and were the target of Au-U mineral prospecting surveys in the 1970s (Lindsey 1975, Villaça 1981, Villaça and Moura 1981, Minter *et al.* 1990).

Due to its siliciclastic nature, preservation, continuity and economic interest, recent detailed sedimentological surveys highlighted new information about the depositional environments and tectonic history of the Moeda basin in the Caraça ridge (Nunes 2016) and the Moeda plateau (Madeira *et al.* 2019). These studies also aggregated robust U-Pb geochronological data performed on detrital zircon and played a significant role in the provenance investigation of the Moeda Formation (e.g., Machado *et al.* 1996, Hartmann *et al.* 2006, Koglin *et al.* 2014, Nunes 2016, Dopico *et al.* 2017).

[1]Departamento de Geologia, Escola de Minas, Universidade Federal de Ouro Preto – Ouro Preto (MG), Brazil. E-mails: madureira.geo@gmail.com, maximilianomartins@yahoo.com.br, glauciaqueiroga@yahoo.com.br, cristianodeclana@gmail.com, ana_alkmim@yahoo.com.br

[2]Instituto Federal de Minas Gerais – Governador Valadares (MG), Brazil.

[3]Instituto de Geociências, Universidade de São Paulo – São Paulo (SP), Brazil. E-mail: luizdutra@usp.br

*Corresponding author.

This paper aimed to fill the gap in the sedimentary evolution and provenance approach of the Moeda Formation in the Southernmost Gandarela and Ouro Fino synclines, Central-Eastern QF. Both segments preserve early and late syn-rift deposits of the Moeda Formation and were postulated as remaining individual half-grabens of the Moeda rifting zone, separated by a structural high and bounded by reactivated thrust-reverse faults (Madureira 2020). We present a sedimentological and stratigraphic analysis on the Moeda Formation metasedimentary sequences at its maximum thickness areas (Lindsey 1975), combined with U-Pb detrital zircon dating on key stratigraphic intervals. Furthermore, a paleoenvironmental reconstruction is presented, integrating the analysis of preserved sedimentary records, depositional systems, and ages of main source rocks.

GEOLOGICAL SETTING

The QF is located in the Southeastern edge of the São Francisco Craton (SFC), bordering the Araçuaí orogen (Fig. 1A), (Almeida 1977, Alkmim and Marshak 1998, Alkmim and Martins-Neto 2012, Lana *et al.* 2013, Queiroz *et al.* 2019). The QF was affected by two superimposed orogens:

- Paleoproterozoic Minas orogeny (2100–1900 Ma; Teixeira *et al.* 2015), also known as Transamazonian orogeny (Alkmim and Marshak 1998), which resulted from the collisional events between the cores of both Congo and São Francisco cratons (Fig. 1A; Teixeira *et al.* 2015, Farina *et al.* 2016, Aguilar *et al.* 2017);
- Brasiliano orogeny (700–450 Ma), responsible for the reactivation of Archean to Paleoproterozoic structures,

generating west-verging thrust faults (e.g., Endo and Machado 2002).

The Brasiliano orogeny was responsible for the development of the Fundão-Cambotas fault system, (Endo and Fonseca 1992), which stretches along 60 km in an east-verging concave form in the Central-Eastern QF and encompasses the study area (Gandarela and Ouro Fino synclines; Fig. 1B).

The intensity of thrust-fault systems that affected the QF decreases from East to West, resulting in a root zone of the overthrusts at its Eastern border, including the Caraça ridge, whereas the Western limit, which includes the Moeda syncline, represents the least deformed area (Endo and Fonseca 1992, Chemale Jr. *et al.* 1994, Alkmim and Marshak 1998, Alkmim and Teixeira 2017). Consequently, the best exposures and type-area of the earlier syn-rift deposits of the Moeda Formation are located in the Western limb (Wallace 1958, Villaça 1981, Madeira *et al.* 2019).

The QF lithostratigraphic units (Fig. 2) are the Mesoarchean granite-gneiss complexes overlapped by metavolcanosedimentary sequences of the Rio das Velhas Supergroup (RVS) as well as the Paleoproterozoic metasedimentary successions of the MS and the Itacolomi Group (Dorr II 1969, Alkmim and Marshak 1998, Lana *et al.* 2013, Alkmim and Teixeira 2017).

The Mesoarchean crystalline basement complexes (Fig. 2) are composed of a series of tonalite-trondhjemite-granodiorite (TTG) granitoid, gneiss and migmatite. The main periods of magmatic activity and tectonic accretion in QF are Santa Bárbara (SB; ca. 3200 Ma), Rio das Velhas I (RdVI;
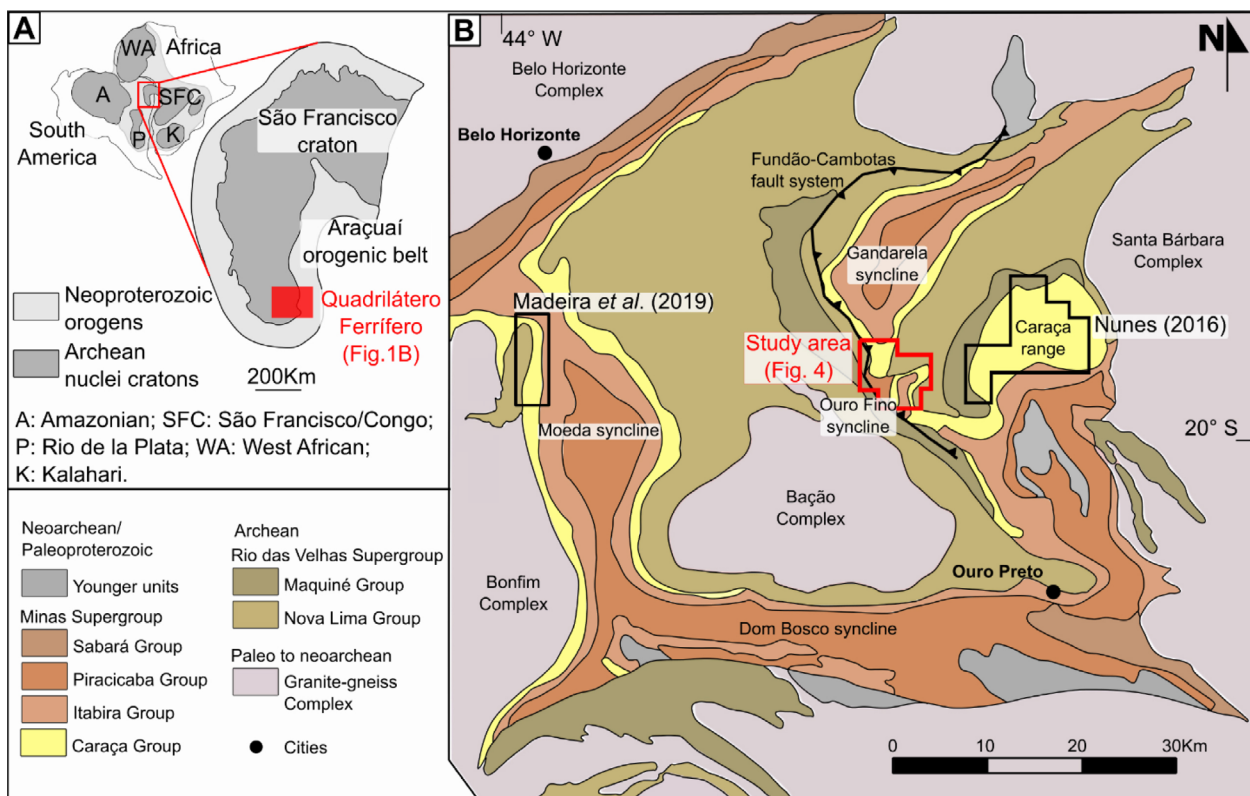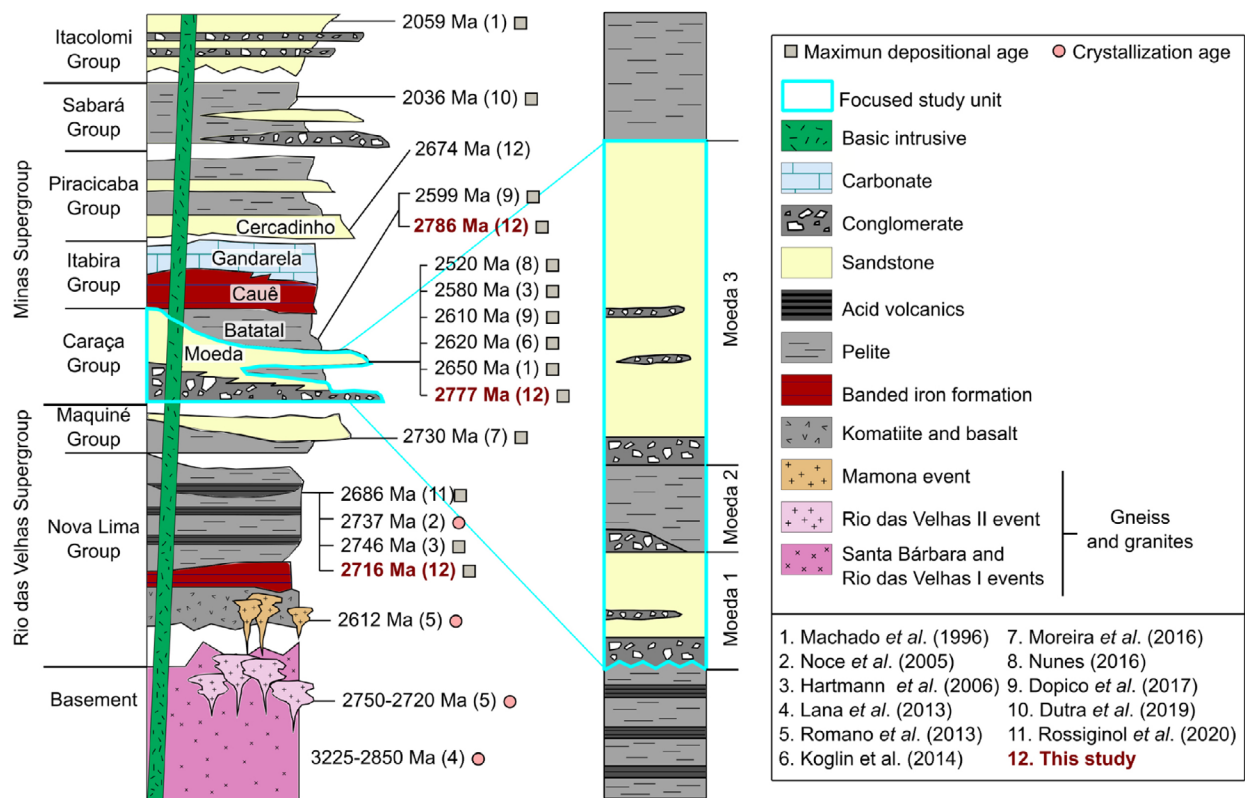

Figure 1. (A) Quadrilátero Ferrífero indicated in the Southern São Francisco Craton in the Western Gondwana geotectonic scenario (based on Renger *et al.* 1994 and Alkmim and Marshak 1998). (B) Simplified geologic map of the Quadrilátero Ferrífero with its main structures.

Source: based on Wallace (1958), Dorr II (1969), Villaça (1981), Alkmim and Marshak (1998) and Dopico *et al.* (2017).

Figure 2. Stratigraphic column of the Quadrilátero Ferrífero and schematic Moeda Formation subdivision. Numbers in parentheses indicate the age data reference listed on figure.

2930–2900 Ma), and Rio das Velhas II (RdVII; 2800–2770 Ma) (Lana *et al.* 2013, Romano *et al.* 2013). Widespread K-rich intrusions mark another magmatic event, subdivided into Mamona I (MI; 2750–2700 Ma) and Mamona II (MII; 2620–2580 Ma) (Romano *et al.* 2013, Farina *et al.* 2015, 2016, Dopico *et al.* 2017). Moreover, Campos *et al.* (2003) described granitic and tonalitic intrusions in the Southern QF related to the Minas accretionary orogeny (2100–1900 Ma).

The Archean RVS (Fig. 2) is composed of metavolcanosedimentary units attributed to a greenstone belt sequence of oceanic to foreland basin (Dorr II 1969, Alkmim and Marshak 1998, Baltazar and Zucchetti 2007). The RVS consists of mafic-ultramafic metavolcanic rocks with intercalation of metapelites (Nova Lima Group), overlapped by a clastic sequence of metaconglomerate and metasandstone from an alluvial-fluvial depositional system (Maquiné Group) (Dorr II 1969, Zucchetti *et al.* 1998, Baltazar *et al.* 2005). The Nova Lima Group's U-Pb crystallization age suggests magmatic activity between 2790 and 2750 Ma (Dopico *et al.* 2017), whereas the youngest detrital zircon population of the Maquiné Group has a maximum depositional age of 2730 ± 18 Ma (Moreira *et al.* 2016).

The Paleoproterozoic MS (Fig. 2) is a metasedimentary package that unconformably overlies the RVS. It comprises the Caraça, Itabira, Piracicaba and Sabará groups; the Tamanduá Group has been definitively excluded as a basal unit of the MS and correlated to the Espinhaço Supergroup instead during Paleo-to-Mesoproterozoic (Dutra *et al.* 2020). The Caraça

Group, focused on herein, comprises alluvial-fluvial metasandstone, metaconglomerate and metapelite (Moeda Formation) and is overlain by metapelites from a shallow marine environment (Batatal Formation) (Dorr II 1969, Alkmim and Marshak 1998). The regional knowledge about stratigraphy and sedimentary facies distribution of the Moeda Formation is mainly due to the papers of Wallace (1958), Dorr II (1969) and Villaça (1981). These authors informally divided the Moeda Formation into three members with variable thickness in the QF (Fig. 2). The basal Moeda 1 member is composed of metaconglomerates with a fine-grained matrix, sericite-rich (often pyrite and/or carbonate), typical of an alluvial depositional system dominated by braided rivers. The intermediate member (Moeda 2) is composed of fine-grained metasandstone and metapelite from a shallow and transgressive marine sedimentary environment. The upper Moeda 3 comprises a package of medium-grained metasandstone with cross-bedding from a fluvial environment. According to Alkmim and Martins-Neto (2012), the entire Moeda Formation is a fourth hierarchical order stratigraphic sequence. Available geochronological data for the Moeda Formation point to a maximum depositional age ranging from 2650 to 2520 Ma (Machado *et al.* 1996, Hartmann *et al.* 2006, Koglin *et al.* 2014, Nunes 2016, Dopico *et al.* 2017). The Batatal Formation maximum depositional age was determined by Dopico *et al.* (2017) as 2559 ± 22 Ma; however, this age is older than the underlying Moeda Formation. Therefore, the depositional age of Batatal Formation is bracketed between 2520 and 2453 Ma, maximum depositional ages of the Moeda Formation and

overlying Cauê Formation proposed by Nunes (2016) and Cassino (2014), respectively.

The Itabira Group consists of banded iron-formation and carbonatic sequences of marine transgression deposited in a tectonic quiescence period, overlapped by marine to deltaic metasandstone and metapelite of the Piracicaba Group (Renger *et al.* 1994, Dutra *et al.* 2019, Rossignol *et al.* 2020). The MS final deposition stage is represented by the siliciclastic units of the Sabará Group, a sin-orogenic succession correlated to the tectonic inversion of the Minas Basin during the Minas orogeny (Dorr II 1969, Renger *et al.* 1994, Alkmim and Marshak 1998, Teixeira *et al.* 2015, Dutra *et al.* 2019).

The Rhyacian Itacolomi Group (Fig. 2) consists of a package of fluvial metasandstone, metaconglomerate and metapelite related to the foreland basin (Dorr II 1969, Alkmim and Martins-Neto 2012) correlated to the Minas orogeny collapse at ca. 2143–1960 Ma (Machado *et al.* 1996, Hartmann *et al.* 2006, Alkmim *et al.* 2014, Duque 2020). Mafic dike swarms intrude the entire QF sequence (Fig. 2), dated at ca. 1.79, 1.71–1.70, 0.90 and 0.70 Ga (Silva *et al.* 1995, Cederberg *et al.* 2016).

Local background

The Gandarela and Ouro Fino synclines are located in the culmination of the hanging wall of the Fundão-Cambotas thrust fault (Fig. 1B) (Endo and Fonseca 1992), and they were not affected by dome emplacement tectonics at the end of Transamazonian orogeny (Alkmim and Marshak 1998). Therefore, this area preserves, at least, part of the thin-skinned tectonics of the superimposed Transamazonian and Brasiliano events, with variable degrees of intensity (Chemale Jr. *et al.* 1994, Alkmim and Marshak 1998).

Based on geological mapping conducted at scale 1:10.000, Madureira (2020) and references therein describe the main structural features and boundary contacts of the Moeda Formation, justifying the location of the eight logs used to identify the lithofacies associations of this unit (Fig. 3).

The Western contacts of the Moeda Formation, in both the Gandarela and Ouro Fino synclines, are evidenced by fault zones (Fig. 3), which exhibit NE-SW-striking mylonitic foliation, dipping Southeast, and kyanite and white mica as sin-tectonic minerals.

The Southern segment of the Gandarela syncline is a NE-SW-trending homocline structure (Fig. 3). Sedimentary bedding and penetrative foliation are along-strike oriented and show a dip Southeast. From West to East at the Gandarela syncline, the Moeda Formation overlies the Nova Lima Group by a basal detachment fault and is top limited by a paraconformity surface with the metapelites of the Batatal Formation (Madureira 2020).

In the domain of the Ouro Fino syncline, the siliciclastic succession of the Moeda Formation overlays the Batatal Formation through a reverse fault (Fig. 4). This reverse fault characterizes the front of Ouro Fino syncline thrust system. Through map view, this fault is arc-shaped, concavity facing East (Fig. 3) and controls the distribution of the NE-SW-striking bedding and mylonitic foliation.

MATERIALS AND METHODS

Our study focuses on the sedimentary evolution and U-Pb detrital zircon geochronology provenance of syn-rift units in the Moeda Formation. We used geological mapping at a scale of 1:10,000 (Madureira 2020) and high-resolution satellite imagery from Google Earth as base maps in order to guarantee accuracy regarding the logs' location. We analyzed eight detailed logs from short cross-sections located at a preserved stratigraphic sequence of the Moeda Formation, previously controlled by local structural geology (as seen in the "Local background" topic and Fig. 3).

Eight logs were performed at a scale of 1:200, reaching 1,490 m. These logs were oriented parallelly to the dip direction. The upper paraconformity contact with metapelites of Batatal Formation, the overlapping Moeda Formation unit, was considered as the upper stratigraphic datum. Jacob's staff was used to correct dip and to measure the true stratigraphic thickness, as described by Miall (2016). Due to low-grade metamorphism and well-preserved primary features of strata in the Moeda Formation, sedimentary terminologies were used for facies descriptions in the field and laboratory, as proposed by Miall (1996), Tucker (2001), Stow (2005) and Boggs (2009). Eight thin polished sections were described under a ZEISS microscope, and all photomicrographs were taken by the AxioCam Erc5s at the Department of Geology, Universidade Federal de Ouro Preto (DEGEO/UFOP, Brazil). The abbreviations for mineral names act in accordance with Whitney and Evans (2010).

Detrital zircon grains were separated from six rock samples collected in key stratigraphic intervals in the Moeda and Batatal formations (Caraça Group, MS) and the Nova Lima Group (RVS), representing the top and bottom limits of Moeda Formation, respectively. The extraction and concentration of zircon grains were conducted at the Sample Preparation for Geochronology Laboratory (DEGEO/UFOP) through conventional methods (crushing, grinding gravimetric, Nd-magnet and magnetic-Frantz separator). Additionally, separation using heavy liquid (bromoform — 2,89 g/cm^3) was conducted. For each sample, around 200 zircon grains were handpicked under a binocular microscope. Grains were placed on an epoxy mount (SpeciFix, 25mm), polished to expose their cores. Grains were scanned using cathodoluminescence (CL) to reveal zoning, internal fractures, inclusions, as well as the core and rim structure. CL images were obtained via scanning electron microscope (JEOL JSM-6510), under 20 kV, in the Microscopy and Microanalysis Laboratory (DEGEO/UFOP).

U-Pb isotopic analyses were carried out in an Inductively Coupled Plasma – Mass Spectrometry (ICP-MS) Thermo Scientific Element 2 coupled to a CETAC LSX-213 laser abrasion system in the Isotope Geochemistry Laboratory (DEGEO/UFOP). For each analysis, the initial 30 ms of laser abrasion were discarded and assessed as background information, considering only the 30 ms subsequently data obtained. The laser was fired using 30 µm spot size, energy of 2.04 J/cm^2 and a frequency of 10 Hz. BB (Santos *et al.* 2017), GJ-1 (Jackson *et al.* 2004) and Plešovice (Sláma *et al.* 2008) zircons were used as reference materials for the Laser Ablation – Inductively Coupled Plasma – Mass Spectrometry (LA-ICP-MS) analytic routine.
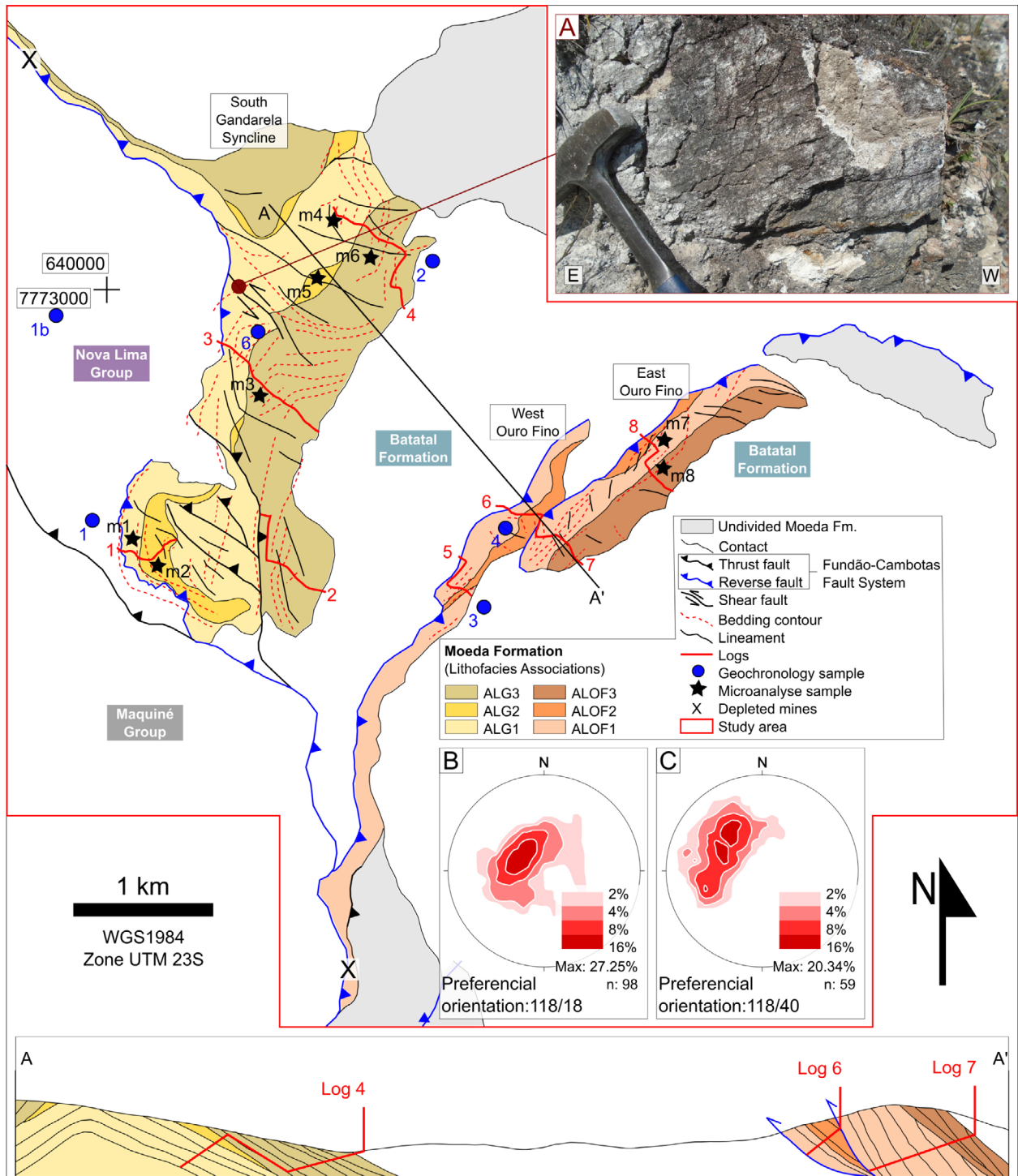
Figure 3. Lithofacies association map of Southern Gandarela and Northern Ouro Fino synclines. (A) Shear fault steps with sinistral movement. (B) Sedimentary bedding (S0) pole density diagram for the Moeda Formation lithologies at the Southern Gandarela syncline. (C) Bedding (S0) pole density diagram of Moeda Formation rocks at Northern Ouro Fino syncline.

Data reduction was performed using the Glitter software (van Achterbergh *et al.* 2001). The ages considered present a maximum discordance of 5%, standard deviation of up to 2.5% and Th/U ratio greater than 0.1, which ensure a non-metamorphic origin for the crystals (López-Sanchéz *et al.* 2016). The results of the LA-ICP-MS analyses are reported in the Supplementary Table A1.

The probability density diagrams, concordia and average ages were generated from ^{207}Pb/^{206}Pb ratios, with error 2σ, via Isoplot 4.15 (Ludwig 2012) implemented to Microsoft Excel.

LITHOFACIES AND LITHOFACIES ASSOCIATIONS

Nine sedimentary lithofacies were characterized in the Moeda Formation (Tab. 1) and grouped into six lithofacies associations (Fig. 5). The entire Moeda Formation represents the fourth hierarchical order stratigraphic sequence (Alkmim and Martins-Neto 2012), therefore its nested stratigraphic fining and coarsening upward cycles, herein identified, consist of lower-hierarchical order stratigraphic sequences. The Moeda Formation lithofacies associations
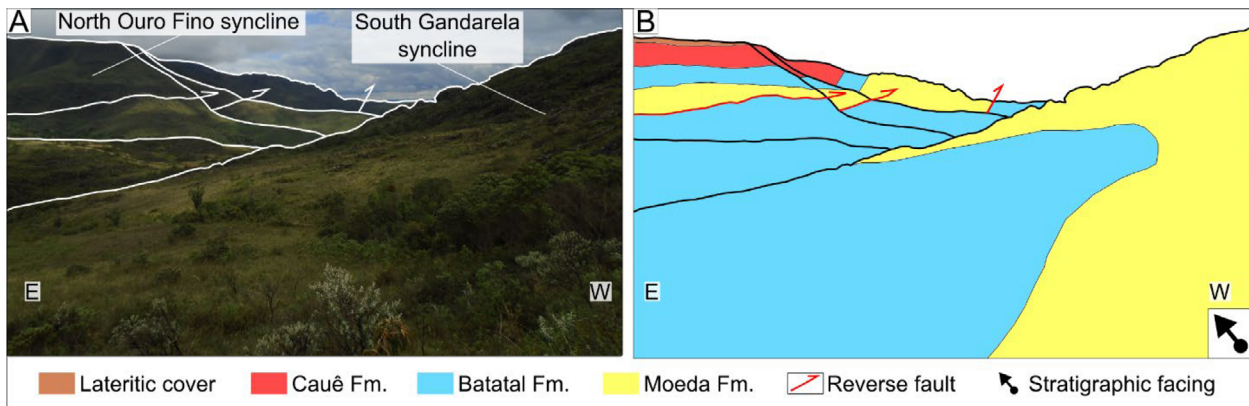
Figure 4. (A) General morphology of the Southern Gandarela and Northern Ouro Fino synclines. (B) Schematic profile showing the distribution of the Caraça Group (Moeda and Batatal formations) and Itabira Group (Cauê Formation) in the Minas Supergroup. View to South (640857/7771545, WGS 1984 Zone 23S).

were designed as ALG1, ALG2 and ALG3 in the Southern Gandarela syncline, and ALOF1, ALOF2 and ALOF3 in the Ouro Fino syncline (Tab. 2). Although there are similarities in the lithofacies associations from both synclines, they were described and interpreted separately as an effort to avoid precocious and dubious correlations regarding their depositional sedimentary systems.

In order to better describe the distribution and thickness of the lithofacies associations in the Ouro Fino syncline, the NE and SE structures that compose its Northern portion were referred to as West Ouro Fino and East Ouro Fino (Figs. 3 and 5).

Lithofacies association – ALG1

The ALG1 (Tab. 2 and Fig. 6A) is composed of massive oligomict conglomerate beds (lithofacies Cms, CcsI, CcsII) and coarse- to very coarse-grained sandstone (lithofacies Amg, Ammg, Acd; Tab. 1). The conglomerate beds are predominant and presented in tabular geometry of up to 9 m-thick. The sandstone occurs interbedded with the conglomerate in lenses and bodies of up to 2.0 m-thick. The ALG1 presents its maximum thickness in the Southernmost Gandarela syncline, which reaches 75 m-thick (Log4; Figs. 3 and 5). This lithofacies association is bottom limited by a nonconformity, a partially tectonized contact with quartz-chlorite-sericite schist of the Nova Lima Group and top limited by gradual conformity with the sandstones in the ALG3, or occasionally, medium-grained sandstones of the ALG2 (Fig. 5).

The conglomerate beds are clast- to matrix-supported with clast sizes ranging from 0.5 to 20.0 cm in diameter, consisting of milky and smoky quartz and quartzite with smoky quartz grains. Optical microscopy analyses of Amg lithofacies (sample m1; Fig. 5) and conglomerate matrix of ALG1 (sample m4; Fig. 5) indicate a composition of 10–15% matrix and 85–90% grains (Fig. 6B). The framework grain is made up of monocrystalline quartz and fragments of fine- to coarse-grained quartzite and chert. The matrix is composed of clay minerals, which consists of protomatrix (95%) and pseudomatrix (5%). The Amg and conglomerate matrix of ALG1 is moderately to poorly sorted and texturally immature, in which grains are subangular and exhibit low-to medium sphericity.

The ALG1 exhibits the sixth hierarchical order fining upward sedimentary cycles of 4.0 to 23.0 m-thick, which are constituted by oligomict conglomerates grading from coarse-to very coarsely-grained sandstones (Fig. 5). The cyclic recurrence of the sixth hierarchical order sequences defines a stacking pattern of lower and higher hierarchy, a fifth hierarchical order, coarsening and thickening upward cycle (sandstone predominance grading to massive conglomerate predominance) of about 40 m-thick (Fig. 5).
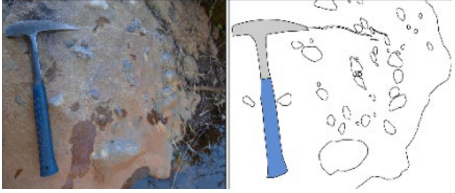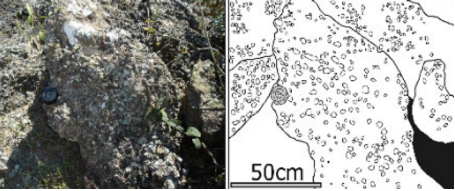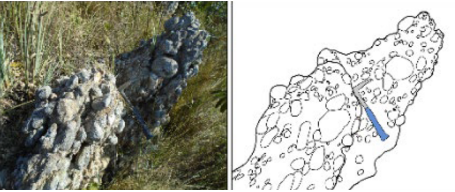
Lithofacies association – ALG2
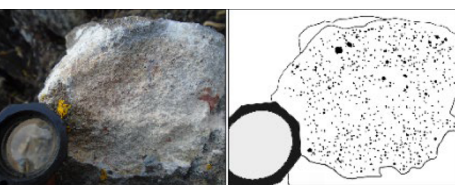
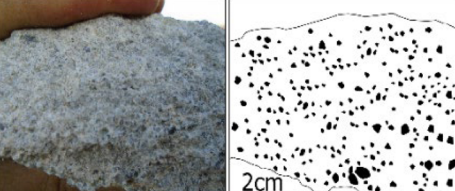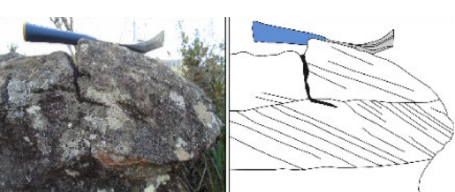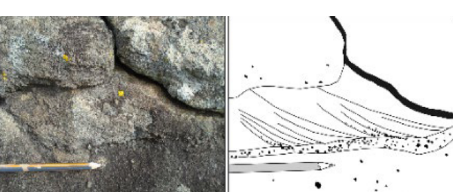The ALG2 (Tab. 2 and Fig. 6C) encompasses massive fine-to medium-grained quartzarenites (Amm lithofacies; Tab. 1) and lenses of massive medium- to coarse sandstones (Amg lithofacies; Tab. 1). The ALG2 does not have lateral continuity (Figs. 3 and 5) and presents its maximum thickness in the Southernmost Gandarela syncline, which reaches 46 m-thick (Log 1; Fig. 5). The ALG2 is bottom and top limited by gradual conformity contacts, mainly ALG1 conglomerates at the base and ALG3 very coarse-grained sandstone on top (Figs. 3 and 5).

The framework grain of the Amm and Amg lithofacies is mostly composed of monocrystalline quartz followed by minor proportions of quartzite and chert fragments. Optical microscopy analysis of the Amm lithofacies show a 97% grains and 3% matrix composition (samples m2 and m5; Figs. 5 and 6D). The clay minerals in this lithofacies association matrix cover partially the quartz grains surface (Fig. 6D). The Amm lithofacies is moderately well-sorted and texturally sub-mature, with subangular-to angular low sphericity grains.

Lithofacies association – ALG3

The ALG3 (Tab. 2 and Fig. 6E) consists of massive, planar, and tangential cross-bedded coarse- to very coarse-grained sandstones (lithofacies Ammg, Apmg, Atmg, respectively; Tab. 1) and massive oligomict conglomerates (lithofacies Cms, CcsI, CcsII; Tab. 1). The sandstone beds are predominant and presented in tabular geometry up to 35 m-thick. The conglomerate occurs interbedded and in geometry of lenses to bodies up to 7 m-thick (Log 3; Fig. 5). The ALG3 presents its maximum thickness in Log 3, which reaches 218 m-thick (Figs. 3

Table 1. Main sedimentary features and interpretations of the Moeda Formation lithofacies at Gandarela and Ouro Fino synclines.

| Lithofacies	Description	Processes	Picture/sketch
Cms	Massive matrix-supported conglomerate with angular pebbles to cobbles (1–18 cm) and moderately sorted quartz sandy matrix	Plastic (laminar) debris flow	
CcsI	Massive clast-supported conglomerate with coarse- to very coarsely-grained matrix. Clasts are angular to sub-rounded pebbles (0.5–4 cm)	Debris flow (turbulent) or fluvial bed load	
CcsII	Massive clast-supported conglomerate with angular to sub-rounded pebbles to cobbles (1–20 cm)	Debris flow (turbulent) or fluvial bed load	
Amm	Massive, fine- to medium-grained, moderately to well sorted sandstone	Sediment-gravity flow	
Amg	Massive, medium- to coarsely-grained moderately sorted sandstone	Sediment-gravity flow	
Ammg	Massive, coarse to very coarsely-grained, poorly sorted sandstone. Rare granule clasts.	Sediment-gravity flow	
Apmg	Coarse- to very coarsely-grained, poorly sorted sandstone with medium-scale and high-angle planar cross-stratification. Rare granule clasts.	Straight-crested (2D) dunes or transverse bar	
Atmg	Coarse- to very coarsely-grained, poorly sorted sandstone with medium-scale and high-angle tangential cross-bedding.	Sinuous-crested and linguoid (3D) dunes or transverse bar	
Acd	Massive, coarse- to very coarsely-grained, moderately sorted sandstone	Plastic (laminar) debris flow	
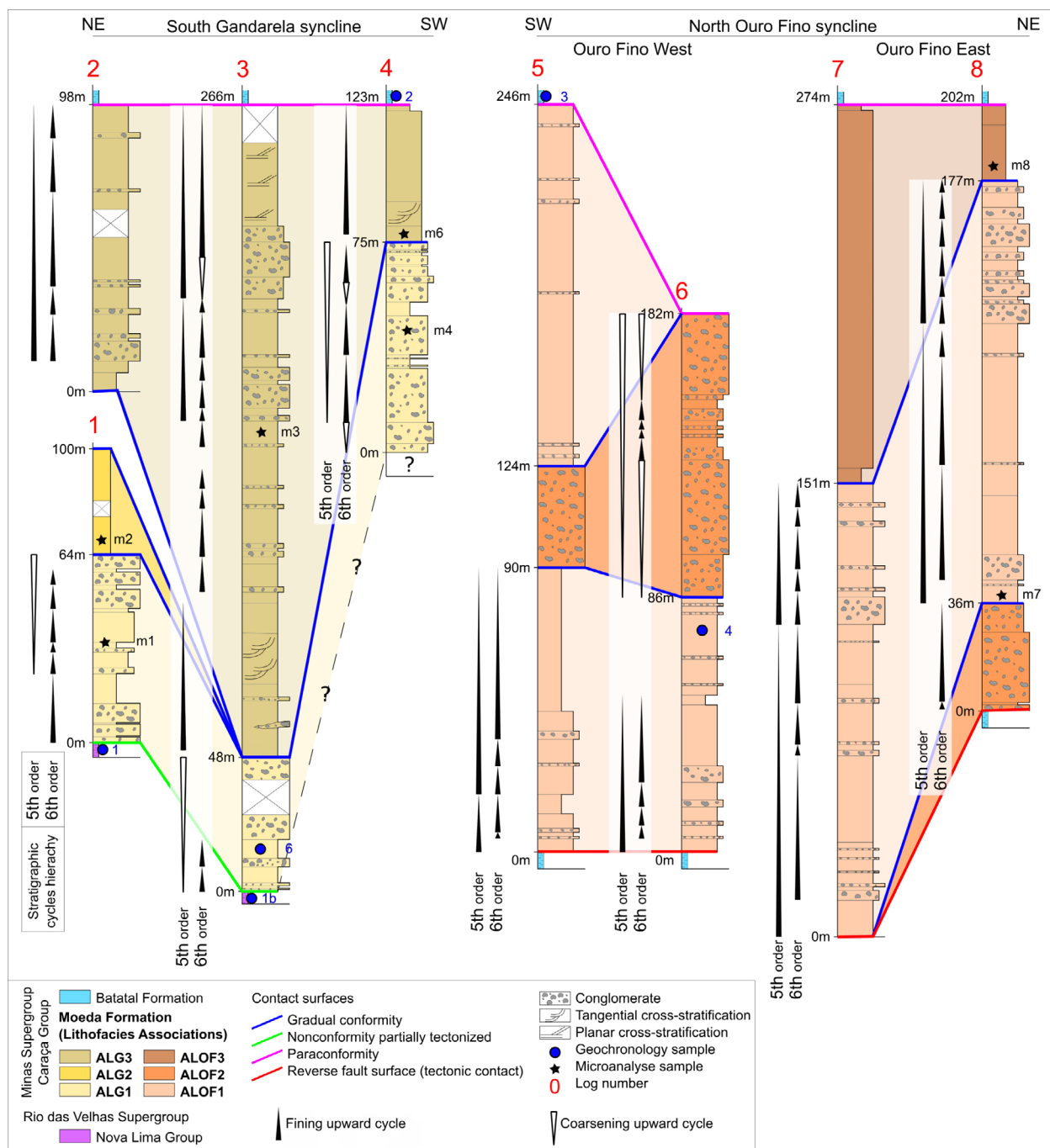
Figure 5. Stratigraphic logs on the Moeda Formation in the Southern Gandarela and Northern Ouro Fino synclines showing lateral lithofacies association correlations with their respective hierarchical order of stratigraphic cycles.

and 5). This lithofacies association is bottom limited by gradual conformity with the massive conglomerates in ALG1, and it is top limited by a paraconformity with the Batatal Formation metapelites (Fig. 5).

The sandstone lithofacies of the ALG3 are predominantly massive (Ammg) with minor planar (Apmg) and tangential cross-bedded (Atmg), both at medium scale. Optical microscopy analyses of Ammg lithofacies (samples m3 and m6, Ammg; Fig. 6F) show a 80% grain and 20% matrix composition. The framework grain consists of monocrystalline quartz, coarse- to fine-grained quartzite fragments as well as minor white mica and rutile. The matrix is clayey to sandy and extremely heterogeneous (Fig. 6F). The Ammg lithofacies of the ALG3 is texturally immature with low sphericity, angular grains.

The ALG3 presents the sixth hierarchical order fining upwards sedimentary cycles of 6.0 to 45.0 m-thick. These stratigraphic cycles are made of massive oligomict conglomerates at the base, grading to the sandstone lithofacies on top. The stacking pattern of the entire ALG3 exhibits the fifth hierarchical order fining upward sedimentary cycles of 41.0 to 98.0 m-thick (Fig. 5). The ALG3 conglomeratic lithofacies presents a decrease in clast content towards the top of Log 2 and a complete absence in Log 4 (Fig. 5).

Lithofacies association – ALOF1

The ALOF1 (Tab. 2 and Fig. 7A) encompasses massive medium- to coarse-grained and coarse- to very coarse-grained sandstones (lithofacies Ammg, Amg; Tab. 1) with

Table 2. Description and interpretation of the Moeda Formation's (Minas Supergroup) lithofacies associations observed in the Gandarela and Ouro Fino's synclines.

Study areas	Lithofacies association	Dominant and (subordinated) lithofacies	Description	Sedimentary environment
Gandarela Syncline	ALG1	CcsI, Cms, CcsII (Amg, Ammg, Acd)	Matrix- and clast-supported oligomict conglomerate (CcsI, Cms and CcsII) in tabular beds of up to 9.0 m thick and 8.0 m width. Intercalation of coarse- (Amg) to very coarsely-grained (Ammg) sandstone in metric tabular (2.0 m) and centimetric lenticular bed. Fining-upward minor cycles, and an overall decametric coarsening-upward. Clasts are whitish, smoked quartz and quartzite with smoked quartz grains.	Proximal zone in the alluvial fan system dominated by debris flow
	ALG2	Amm (Amg)	Massive quartzarenites (97% quartz and 3% clay minerals) fine- to medium-grained and lenses of coarse- to medium-grained sandstone. Presence of infiltrated clay.	Sheet flow of alluvial floodplain
	ALG3	Ammg, Apmg, Atmg (Cms, CcsI, Amg, Acd, CcsII)	Coarse- to very coarsely-grained sand in tabular beds. Occasional presence of tabular and lenticular conglomerate bed intercalations. Sandstones are massive (Ammg), planar (Apmg) or cross-stratified (Atmg). Conglomeratic intercalations (Cms, CcsI and CcsII) are up to 7.0 m thick, reducing the number of clasts and thickness to the top. Fining-upward sequence. Heterogeneous and poorly sorted clayey- to sandy matrix.	Fluvial fan system dominated by braided rivers with gravel bars
Ouro Fino Syncline	ALOF1	Ammg, Amg (CcsI, CcsII)	Massive coarse- to very coarsely-grained sandstone of up to 60.0 cm thick with a clast supported conglomerate as tabular or lenticular beds. Sandstone/conglomerate intercalations register a fining upward sequence. Clasts are made up of quartz, chert and quartzite fragments as subangular form. Poorly sorted matrix (ca. 60% silt/sand and 40% clay).	Proximal fluvial fan system dominated by braided rivers
	ALOF2	CcsII, CcsI (Ammg)	Massive clast-supported conglomerate predominance at 60.0 cm thick and 2.0 m width lenticular beds of coarse-to-very coarsely-grained sandstone. Metapelite, quartz and quartzite clasts. The conglomerate is poorly sorted, and the clasts are non-oriented.	Alluvial fan system dominated by debris flow
	ALOF3	Ammg, Amg	Massive poorly-sorted coarse- to very coarsely-grained sandstone with tabular and centimeter lenticular beds of medium to coarse-grained sandstone. Occasional presence of a 0.5 cm thick lens of quartz granules. Presence of infiltrated clay and pseudomatrix.	Terminal fan (distal zone of fluvial fan system)

intercalations of oligomict clast-supported conglomerates (lithofacies CcsI, CcsII; Tab. 1). The Ammg lithofacies (massive coarse- to very coarsely-grained sandstone) is predominant and occurs in beds of up to 77.0 m-thick. The clast-supported conglomerates occur in tabular geometry in thin beds of up to 60.0 cm-thick. The ALOF1 is bottom limited by the reverse fault surface (tectonic contact) with the Batatal Formation metapelites, and top limited by a gradual conformity with the ALOF2 clast-supported conglomerates and massive sandstones of ALOF3, or by paraconformity with metapelites of Batatal Formation.

Optical microscopy analyses of Ammg lithofacies of the ALOF1 (sample m7; Figs. 5 and 7B) indicate a 78% grain and 22% matrix composition. The framework grains consist of subangular and low-to moderate sphericity monocrystalline quartz, chert and quartzite fragments. The matrix is heterogeneous, composed of 60% sandy and 40% clayey grains.

The ALOF1 presents the sixth hierarchical order fining upwards sedimentary cycles of 3.0 to 56.0 m-thick, constituted by massive oligomict clast-supported conglomerates, which grading to massive coarse- to very coarse-grained and medium- to coarse-grained sandstones lithofacies. The cyclic recurrence of the sixth hierarchical order sequences defines the fifth order fining upward sedimentary cycles of about 19.0 to 104.0 m-thick (Fig. 5).

Lithofacies association – ALOF2

The ALOF2 (Tab. 2 and Fig. 7C) consists of a predominantly massive clast-supported conglomerate (lithofacies CcsI, CcsII; Tab. 1) with rare massive coarse- to very coarse-grained sandstone lenses (lithofacies Ammg; Tab. 1), which reach up to 60.0 cm-thick and 2.0 m-width. The ALOF2 presents its maximum thickness (95.0 meters) in the Log 6 (Fig. 5). In the West Ouro Fino, the ALOF2 is bottom and top limited by gradual conformity with the massive sandstones of the ALOF1. Exceptionally in the East Ouro Fino, ALOF2 is bottom limited by a high-angle (> 45°) reverse fault surface (tectonic contact) with the Batatal Formation metapelites (Figs. 3 and 5).

The detailed textural and composition parameters of CcsI and CcsII lithofacies can be seen in the "Lithofacies association ALG1" topic and Tab. 1. Exceptionally, the massive clast-supported lithofacies of the ALOF2 in Log 5 contains dark gray metapelites clasts (Fig. 7D). The detailed textural and composition parameters of the massive coarse- to very coarse-grained sandstones lithofacies (Ammg) can be seen in the "Lithofacies association ALG1" topic and Table 1.

The ALOF2 presents the sixth hierarchical order coarsening-upward cycle predominance reaching from 27.0 to 46.0 m-thick. These stratigraphic cycles are constituted by clast-supported conglomerates with 4.0 cm clast diameter grading to clast-supported conglomerates of 20.0 cm-diameter clasts
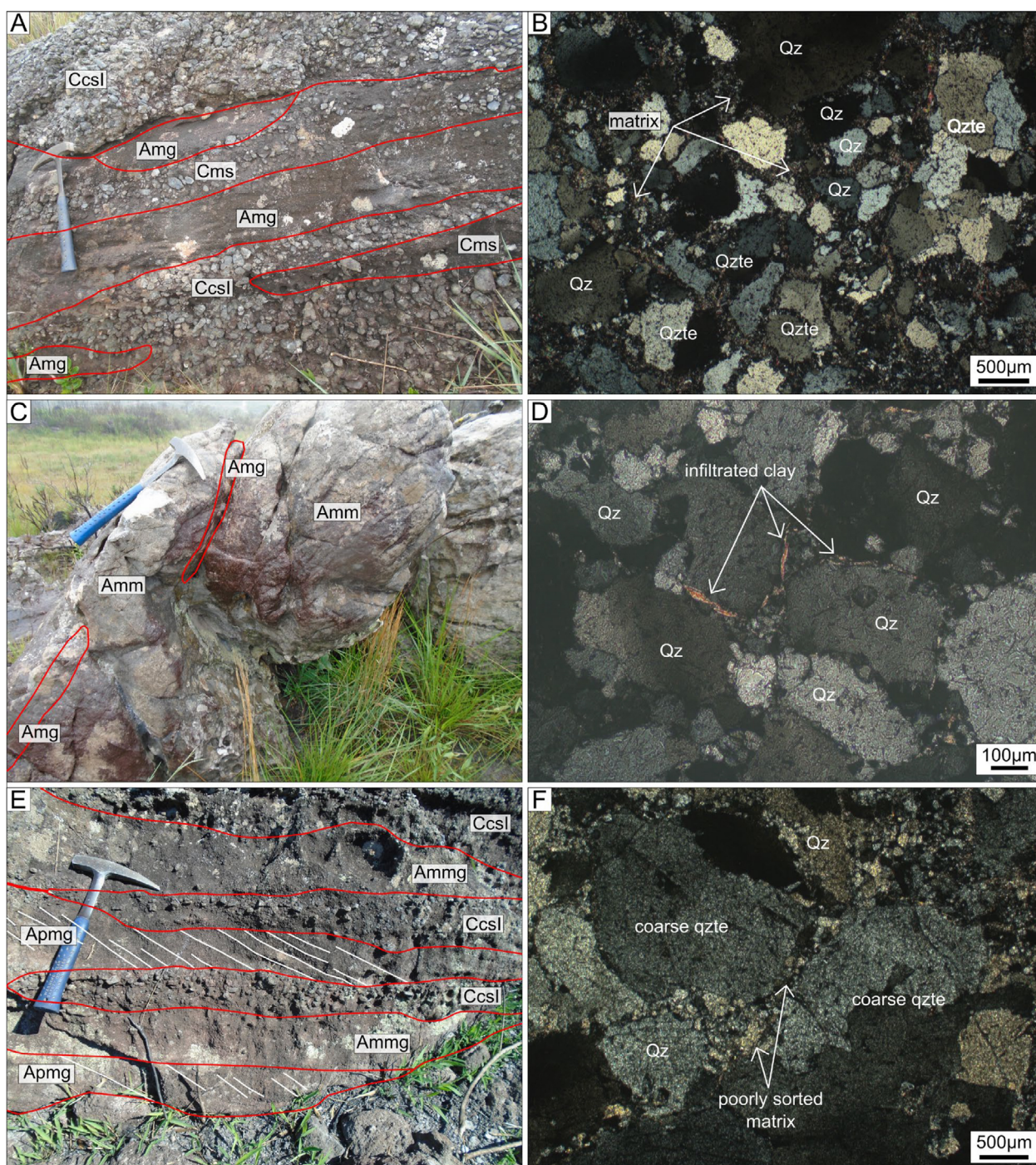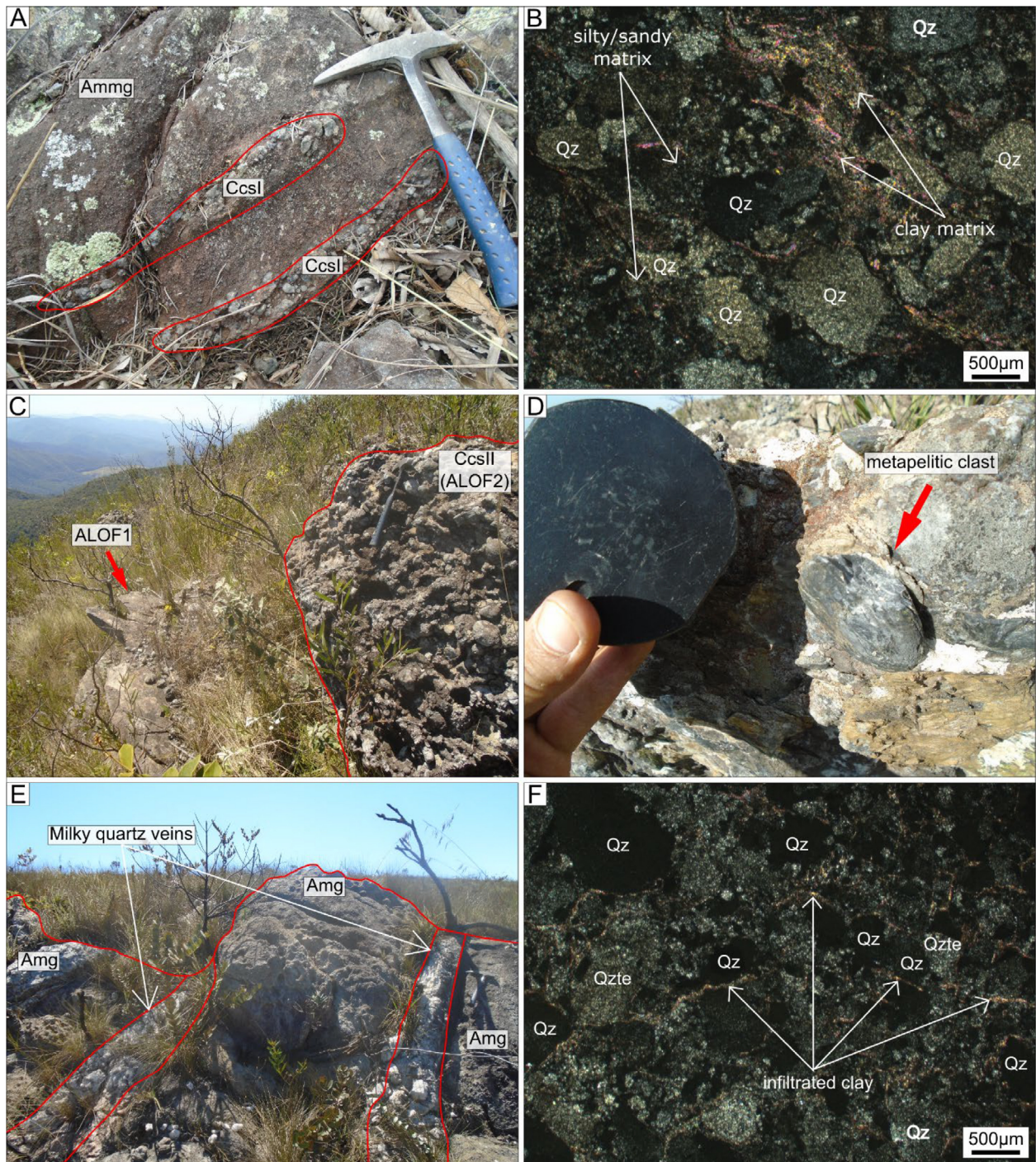
Qz: quartz; Qzte: quartzite.

Figure 6. Lithofacies associations in the Gandarela syncline. (A) Intercalation of conglomerate and massive sandstone of ALG1. (B) Fotomicrography of Amg lithofacies of ALG1 showing the main fabric composition and matrix. (C) Fine- to medium-grained quartzarenite with lenses of massive medium- to coarse sandstones of ALG2. (D) Amm lithofacies microscopic image of ALG2 indicating quartz as the main fabric and infiltrated clay as the matrix. (E) Massive and planar cross-stratified sandstone with clast-supported conglomerate intercalations of ALG3. (F) Fotomicrography of Ammg lithofacies of ALG3 with clayey to sandy matrix. Lithofacies labels are listed in Table 1.

(Fig. 5). The overall stacking pattern of the ALOF2 exhibits a fifth hierarchical order coarsening-upward cycle of 96 m-thick represented by a clast coarsening-upward of its clast-supported conglomerate lithofacies (Fig. 5).

Lithofacies association – ALOF3

The ALOF3 (Tab. 2 and Fig. 7E) consists of massive coarse-to very coarse-grained sandstones and medium-to coarse-grained quartzarenites (lithofacies Ammg, Amg, respectively; Tab. 1). The massive coarse-to very coarse-grained sandstone lithofacies (Ammg) are predominant in the ALOF3 and are presented in beds of up to 116 m-thick (Log7; Fig. 5). The medium-to coarse grained massive quartz-arenites (Amg lithofacies) occur in centimetric lenses and tabular beds of up to 25.0 m-thick. The ALOF3 is bottom limited by gradual conformity with massive sandstones of ALOF1 and top limited by a paraconformity with metapelites of the Batatal Formation.

Qz: quartz; Qzte: quartzite.

Figure 7. Lithofacies associations in the Ouro Fino syncline. (A) Massive coarsely- to very coarsely-grained sandstone with lenticular beds of clast-supported conglomerate of ALFO1. (B) Fotomicrography of Ammg lithofacies of ALOF1 with silt/sand and clay matrix. (C) Contact of clast-supported conglomerate of ALOF2 at the top and ALOF1 at the base. (D) Metapelitic clast of a clast-supported conglomerate of ALOF2. (E) Outcrop of massive medium- to coarsely-grained sandstone of ALOF3 with ca. 40.0 cm thick milky quartz veins. (F) Fotomicrography of Amg lithofacies of ALOF3 showing infiltrated clay as the matrix and quartz as the main fabric. Lithofacies labels are listed in Table 1.

The detailed textural and composition parameters of the Ammg lithofacies can be seen in the "Lithofacies association ALG1" topic and Table 1. Optical microscopy analyses of the Amg lithofacies of ALOF3 indicate a composition of 96% grains and 4% matrix (sample m8; Fig. 7F). Its framework grains consist of monocrystalline quartz, quartzite fragments and subordinate white mica. The quartz grains of this lithofacies are partially covered by clay minerals of the matrix (Fig. 7F). The matrix is also represented by a minor content of pseudomatrix (Fig. 7F). The Amg lithofacies of the ALOF3 are poorly sorted and textural sub-mature, in which grains are angular and exhibit low sphericity.

U-Pb GEOCHRONOLOGY

Detrital zircon U-Pb isotopic analyses were focused on the Moeda Formation (Caraça Group, MS) as an effort to determine its sedimentary provenance based on $^{207}Pb/^{206}Pb$

age distribution diagrams and the youngest age cluster in the Gandarela and Ouro Fino synclines (Fig. 8).

The Batatal Formation (Caraça Group, MS) and the Nova Lima Group (RVS) make up the top and bottom stratigraphic limits of Moeda Formation, respectively. However, these units are composed of similar lithologies and present a stratigraphic inversion in the study area. Therefore, the U-Pb detrital zircon dating was also conducted in the Batatal Formation and Nova Lima Group in order to differentiate and better comprehend the Moeda Formation sedimentary evolution in the Gandarela and Ouro Fino synclines.

The quartz-chlorite-sericite schist of the Nova Lima Group (samples 1 and 1b; Tab. 3 and Fig. 8) contains rounded to euhedral grains in brownish to translucent colors. Fractures within these grains are common. Zircon length ranges from 100 to 300 µm and most of them show $^{232}Th/^{238}U$ ratios between 0.10 and 1.84 (Fig. 8). The age distribution of sample 1b spans from 2764 to 3733 Ma, yielding two main populations at 2764–2994 Ma, and 3071–3248 Ma (Fig 8). The main populations are correspondent to the Rio das Velhas (I and II) and Santa Bárbara magmatic events, which, when combined, constitute 79.8% of the sample 1b concordant ages (n = 75). The age spectrum in sample 1 is remarkably different from sample 1b;

its distribution is unimodal with the main population ranging between 2676 and 3039 (n = 86) (Fig. 8). The Paleoarchean zircons of these samples (3224–3733 Ma, n = 22) predate the first Archean tectono-magmatic event (Santa Bárbara event, ca. 3200 Ma), while 129 zircon ages are not correlated with a known tectono-magmatic event at 2803–3186 Ma (Fig. 8).

The Moeda Formation samples (4 and 6, Tab. 3 and Fig. 8) were collected in the basal sandstone lithofacies (Ammg of ALOF1 and ALG1). Zircon grains are light brown, and most are complete round. Their length ranges from 100 to 400 µm and crystals often exhibit internal fractures (Fig. 8). $^{232}Th/^{238}U$ ratios range from 0.11 to 3.19. The Moeda Formation zircon grains were separated into four groups based on their ages (Fig. 9).

Group I (2722–2872 Ma) consists of dark finely zoned grains and represents 13.8% of the total concordant ages (n = 15) (Fig. 9). Bleached rims in grains 4-56, 4-30 and 6-193 represent dissolution during either metamorphism or hydrothermal alteration and reprecipitation as overgrowths on the core (Vavra *et al.* 1999, Hartmann *et al.* 2000, Harley *et al.* 2007, Grant *et al.* 2009, Rubatto 2017). The dark core of grains 4-56, 4-30 and 6-193 and the entire grain 6-320 are products of enrichment in trace elements during those recrystallization processes (Hoskin and Black 2000).
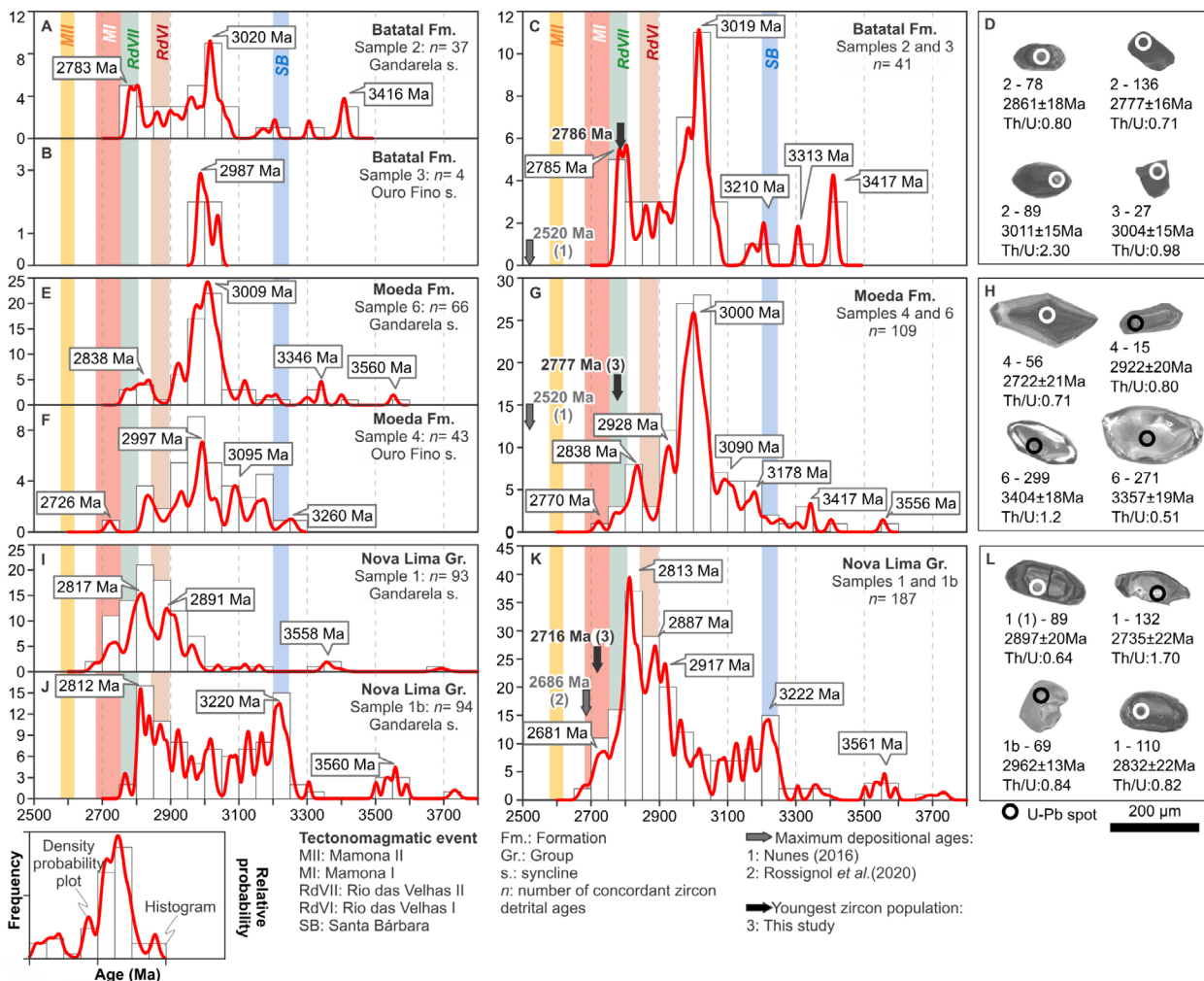

Figure 8. Probability density diagrams of zircon age distribution, youngest age cluster and CL detrital zircon grain images of (A, B, C and D) Batatal Formation; (E, F, G and H) Moeda Formation; (I, J, K and L) Nova Lima Group over the Gandarela and Ouro Fino synclines.

Table 3. Summary of all samples used for zircon U-Pb geochronology.

Samples	Coordinates (WGS 1984 23S)	Number of analyzed zircons (concordant ages)	Unit	Description
3	642647 / 7770755	24 (4)	Batatal Formation	Metapelite
2	642252 / 7773250	117 (37)		
6	641014 / 7772814	140 (66)	Moeda Formation	ALG1 sandstone
4	642791 / 7771271	154 (43)		ALOF1 sandstone
1b	639099 / 7772832	138 (94)	Nova Lima Group	Quartz-chlorite-sericite schist
1	639869 / 7771335	154 (93)		
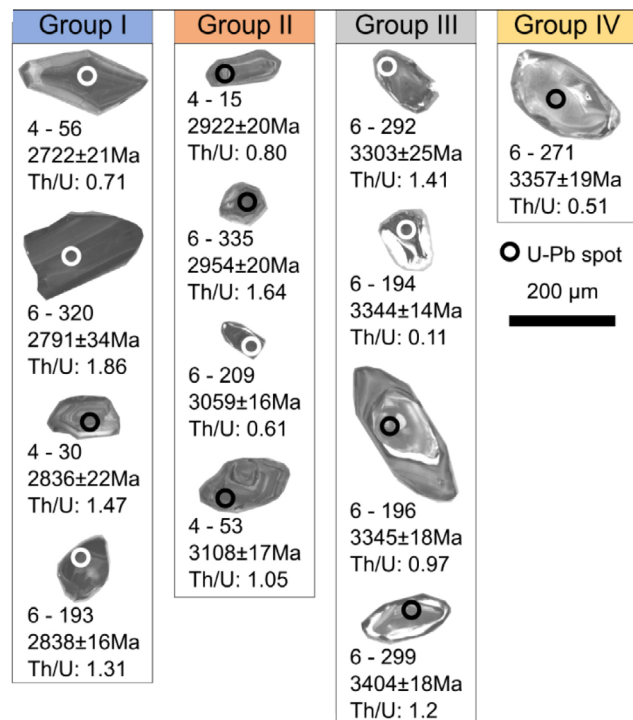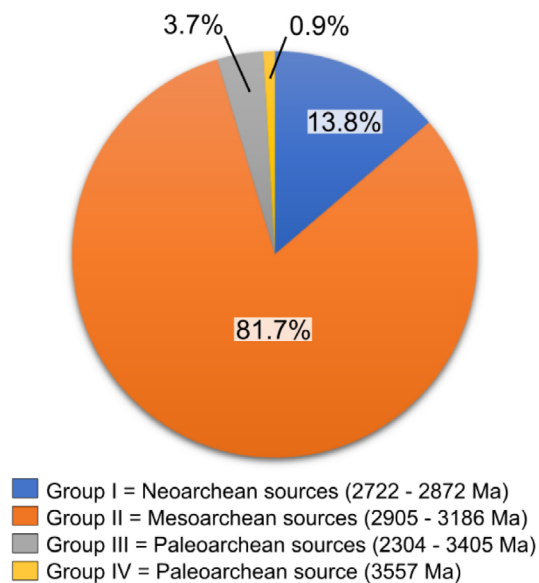
Figure 9. Quantitative proportion and cathodoluminescence images of the Moeda Formation zircon age groups.

Group II (2905–3186 Ma) consists of zircon grains with oscillatory zoning partially preserved in its core, representing 81.7% of the total concordant ages (n=89) (Fig. 9). It is replaced by faint and bright rims associated with the interaction and precipitation of hydrothermal fluids from a melting process, similar to the one occurring in Group I, although the zircons grains in Group II show finer diameters (Fig. 9).

Group III (3304–3405 Ma) shows rounded and subhedral grains and represents 3.7% of the concordant ages (n = 4) (Fig. 9). "Ghost zoning" is associated with the bright inner seam (grains 6-196 and 6-299). Its prismatic-like faces and texture suggest an overprint by recrystallization of existing zircon (Corfu *et al.* 2003, Rubatto 2017). The rounded grain displays partial oscillatory zoning.

The zircon in Group IV (ca. 3557 Ma) displays little or no oscillatory zoning with an bright outer rim and contributes with only one grain in the samples 4 and 6, representing 0.9% of the concordant ages (Fig. 9). These features are common in new zircon growth and recrystallization (Harley *et al.* 2007).

Overall, the age spectrum of the Moeda Formation samples shows a quasi-unimodal distribution with main peaks at 2995 Ma (sample 4; Fig. 8F) and 3013 Ma (sample 6; Fig. 8E).

The secondary population dated at 2722–2872 Ma (n = 15) matches with the Rio das Velhas and Mamona events (Fig. 8).

Samples 2 and 3 were extracted from grayish metapelites of the Batatal Formation (Figs. 3 and 5). Zircon grains are light, dark and reddish brown, which maximal length is 150 μm and ^{232}Th/^{238}U ratio ranges from 0.32 to 2.31. Most grains are prismatic with angular edges, occasionally rounded and rarely fractured (Fig. 8). This unit's detrital age data evidence three main populations (Fig. 8): 2778–2839 (n = 11), 2937–3073 (n = 26) and 3411–3417 Ma (n = 4). These ages are concurrent with the main population of the Moeda Formation and the Rio das Velhas II event (Fig. 8).

DISCUSSION

Interpretations of depositional systems

ALG1 depositional system: proximal zone of alluvial fan dominated by debris flow

The predominance of massive conglomerate beds with sandy lithofacies intercalations indicates high-energy alluvial/

fluvial depositional processes for ALG1, which can be interpreted as gravity debris flow deposit (Tucker 2001, Stow 2005). The low sphericity and subangular grains are indicative of a short transport distance (Tucker 2001, Boggs 2009, Miall 2016). In addition, predominantly coarse-grained sediments tend to occupy proximal zones of sedimentary deposits (James and Dalrymple 2010).

The ALG1 sixth order fining-upward cycles, composed of conglomerates at the base and sandstones at the top, indicate a deposition system of decelerating fluxes with competence reduction (Miall 2010, 2016). The decelerating fluxes can be a result from allogenic controls (e.g., basin-forming tectonism and climate changes) or from autogenic controls, mainly the switching of alluvial channels (James and Dalrymple 2010, Catuneanu 2019). The higher-hierarchical fifth order coarsening and thickening upward cycle (sandstones grading to conglomerates predominance) indicates progradation of the alluvial fans (Assine 2008, Miall 2016).

In this context, the sedimentary environment of ALG1 was interpreted as a proximal zone of an alluvial fan system dominated by debris flow (Tucker 2001, Stow 2005, Assine 2008).

ALG2 depositional system: sheet flow of alluvial floodplain

The presence of clay minerals bordering the quartz grains in the Amm lithofacies of ALG2 (Fig. 6D) indicates a mechanic infiltration (Walker 1992, Boggs 2009). The presence of infiltrated clay suggests the occurrence of an intermittent underwater sedimentary environment, in which infiltration occurs during the water level variations in floodplains, following the deposition of the grains (Boggs 2009). According to Assine (2008), during flood events, static water bodies can be formed in the distal portions of alluvial fans (floodplains) and originate sand sheets without lateral continuity, which can be observed in the area distribution for ALG2 (Fig. 3).

In this context, the ALG2 sedimentation environment is interpreted as sheet flow associated with alluvial floodplain in the distal portions of ALG1 alluvial fans.

ALG3 depositional system: fluvial fan dominated by braided rivers with gravel bars

The presence of planar and tangential cross-beddings sandstones, with conglomeratic intercalations of the ALG3, indicates a fluvial fan depositional system dominated by braided rivers with gravel bars (Reading 1986, Tucker 2001). According to Reading (1986), the tabular geometry of sandstone beds in a fluvial fan system suggests intense lateral migration of the braided channels with commonly gravel bar deposition, which usually results in a sandstone deposit with predominantly conglomeratic lenses, as seen in the ALG3. The fluvial channels lateral migration is also suggested by the sixth order fining-upward sedimentary cycles of the ALG3 constituted by massive oligomict conglomerates grading to sandstone. In addition, the ALG3 fifth order fining-upward sedimentary cycles (conglomerate predominance grading to sandstone predominance) indicate a general stacking pattern of decelerating fluxes with competence reduction (Assine 2008, Miall 2010, 2016).

In this context, we interpreted the ALG3 sedimentary deposition environment as a fluvial fan system dominated by braided rivers (Reading 1986, Tucker 2001).

ALOF1 depositional system: proximal fluvial fan dominated by braided rivers

The heterogeneous matrix, in addition to the subangular and moderate sphericity grains of the ALOF1 sandstone lithofacies, indicates a low-selection fluvial deposition system with short-transport distances (Tucker 2001, Boggs 2009).

The ALOF1 sixth order fining-upward sedimentary cycles (conglomerates grading to massive sandstones) can be a result of intense lateral migration of fluvial braided channels and oscillations in the flow energy (Reading 1986, Assine 2008), while the ALOF1 stacking patterns of the fifth hierarchical order indicate general decelerating flux with competence reduction on its sedimentary transport system (Assine 2008, Miall 2010, 2016).

In this context, we interpreted the ALOF1 sedimentary deposition system as a proximal fluvial fan dominated by braided rivers (Reading 1986, Tucker 2001).

ALOF2 depositional system: alluvial fan dominated by debris flow

Compared to fluvial deposits, alluvial-fan lithofacies associations commonly present a higher competency and proportion of gravel sediments (Reading 1986, Tucker 2001), as seen in the conglomerate predominance in ALOF2. The massive clast-supported conglomerate predominance of the ALOF2 indicates a gravity-induced debris flow deposit (Reading 1986, Boggs 2009, Miall 2016). Debris flows are the dominant sediment-transporting agent in an alluvial fan depositional system (Reading 1986). The sandstone lenses in ALOF2 are a large indicator of constant construction and abandonment of tributary channels, which is typical of an intense lateral migration of the depositional lobes of alluvial fans (Assine 2008). The presence of metapelites clasts in the ALOF2 conglomerate lithofacies indicates at least one proximal source area as a consequence of its low mechanical resistance for long-distance sedimentary transports. The ALOF2 fifth order coarsening-upward cycle, represented by an increase in the clast diameter upward on its clast-supported conglomerates lithofacies, can indicate progradation events of alluvial fans and an increase in the flow competency (Assine 2008, Miall 2016).

In this context, the ALOF2 sedimentary depositional system is interpreted as alluvial fan dominated by debris flow (Reading 1986, Tucker 2001, Boggs 2009, Miall 2016).

ALOF3 depositional system: terminal fan (distal zone of fluvial fans)

The textural sub-maturity of the massive sandstones and quartzarenites lithofacies in the ALOF3 suggests a fluvial fan deposition system (Reading 1996, Tucker 2001, Boggs 2009). The presence of clay minerals bordering the quartz grains (Fig. 7F) indicates mechanic infiltration, which is formally called "infiltrated clays" (Walker 1992, Boggs 2009). The infiltrated clays are indicative of an intermittent underwater sedimentary

environment (Boggs 2009). According to Assine (2008), it can be formed during flood events in distal zones of fluvial fans.

In this context, we interpreted the ALOF3 sedimentary deposition system as a distal zone of the fluvial fan, also known as terminal fan (Reading 1996, Tucker 2001, Assine 2008, Boggs 2009).

Maximum depositional ages

The maximum depositional ages were calculated in the Isoplot 4.15 (Ludwig 2012). This calculation was based on the weighted average age of the youngest clusters of multiple analyses (at least three analyses, n ⩾ 3) with overlapping in age at 2σ (statistical error in millions of years), as proposed by Dickinson and Geherels (2009). This method provides a conservative measure of the depositional age compared to the youngest single grain ages, especially for ancient samples (Dickinson and Geherels 2009, Sharman and Malkowski 2020). These calculated ages were compared with the youngest peak age population of each unit (Tab. 4). Geochronological results of samples from the same unit were integrated in order to increase the frequency of data (n) and, consequently, reduce the uncertainty degree in the calculations of the maximum depositional ages (Fig. 8).

The youngest detrital zircon cluster from the Nova Lima Group indicates a maximum depositional age of 2716 ± 10 Ma, which is slightly older than the available younger age of this unit in the literature (2686 ± 7 Ma; Rossignol *et al.* 2020).

The depositional ages of both the Moeda and Batatal formations (Caraça Group) could not be inferred based on our data. According to the geochronological framework of Moeda and Batatal formations, the major age populations decrease to 2611–2699 Ma (27% of contribution; Rossignol *et al.* 2020). However, ages younger than 2720 Ma were not dated in our samples (Fig. 8). Nonetheless, the depositional age of the Moeda and Batatal formations in the Gandarela and Ouro Fino synclines must be between 2716 Ma, the Nova Lima schist age obtained herein, and 2520 Ma, the depositional age of the Moeda Formation dated by Nunes (2016).

Provenance analysis based on U-Pb detrital zircon dating

The integrated spectrum of ^{207}Pb/^{206}Pb age distribution in the Moeda Formation detrital zircons (Fig. 8G) registers a prominent peak at 3000 Ma, followed by minor peaks at 2770 Ma, 2838 Ma, 3090 Ma, 3178 Ma and 3417 Ma. This distribution suggests that the sediments were derived from the RVS metavolcanosedimentary sequence and from the Bação, Bonfim and Belo Horizonte TTG complexes. The main source, 2905–3186 Ma (Group II; Fig. 9), is most likely a Mesoarchean continental crust that was intensely reworked from the Mesoarchean to Neoarchean. Its presence is indicated by a large number of Mesoarchean detrital grains of both the RVS and MS (c.f., Hartmann *et al.* 2006, Lana *et al.* 2013, Koglin *et al.* 2014, Moreira *et al.* 2016).

The ^{207}Pb/^{206}Pb age distribution spectra of the Batatal Formation (Fig. 8C) display its main peak in the Mesoarchean, between 2937 and 3073 Ma. A secondary peak, 2785 Ma, is correlated to the Rio das Velhas II event. The ^{207}Pb/^{206}Pb age distribution spectra allow us to suggest the felsic intrusions, hosted in the Bação, Bonfim and Belo Horizonte complexes, as likely source areas for the Batatal Formation in the Gandarela and Ouro Fino synclines, similar to those proposed for the Moeda Formation. The third minor peak in our histogram registers the presence of detrital zircons before the Santa Bárbara event, dated at 3417 Ma, indicating the sedimentary contribution of a preexisting crust. The Batatal Formation's maximum depositional age determined by Dopico *et al.* (2017) at the Moeda syncline and the one calculated on this study at the Gandarela and Ouro Fino synclines (Tab. 4) suggest the aging of the source areas from W to E direction of the QF.

Similar source areas suggested for the Moeda and Batatal formations (Caraça Group; MS) are demonstrated in several QF portions by Renger *et al.* (1994), Farina *et al.* (2016) and Dopico *et al.* (2017). These authors also indicated the Archean granite-gneisses complexes of the southern São Francisco Craton as the main source areas for both units.

The chronostratigraphic inversion of the youngest clusters of the Moeda and Batatal formations (Caraça Group, MS — 2777 ± 14 Ma and 2786 ± 9 Ma, respectively) as well as the maximum depositional age of the Nova Lima Group (SRV — 2676 ± 14 Ma), indicate a progressive exhumation of the common source areas (Bação, Bonfim and Belo Horizonte complexes) with contribution from older zircon grains on the Caraça Group basin filling. Comparing the stratigraphic sequences, the younger ages obtained from the Nova Lima Group may be also a result of the detrital zircon contribution from younger K-rich granitoids, generated during the Mamona I event.

Basin filling

Since Wallace (1958), Dorr II (1969), Lindsey (1975), Villaça (1981), Villaça and Moura (1981) and Moraes (1985), two main distinguishable tectono-sedimentary depositional systems became well-established for the Moeda Formation:
- its early basal syn-rift alluvial deposits;
- its upper rift-to passive margin of fluvial to marine deposits, which are top limited by a paraconformity contact of transgressive surface with the overlapped Batatal Formation.

According to the sequence stratigraphy terminologies (Catuneanu 2019), the transgressive surface paraconformity

Table 4. Statistical analysis of U-Pb zircon age populations from samples of the Nova Lima and Caraça groups.

Unit	Youngest grain cluster with n ⩾ 3		Maximum depositional age
	Peak age probability	Weighted mean age	
Batatal Formation	2785 Ma	2786 ± 9 Ma	
Moeda Formation	2770 Ma	2777 ± 14 Ma	2520 ± 13 Ma[1]
Nova Lima Group	2738 Ma	2716 ± 10 Ma	2686 ± 7 Ma[2]

[1]Nunes (2016); [2]Rossignol *et al.* (2020).

can be classified as Transgressive Surface of Erosion. Among the two Moeda Formation tectono-sedimentary depositional systems, various alluvial to fluvial rift-related depositional systems are inferred with their own particularities in each portion of QF. These particularities are reinforced by recent detailed sedimentological surveys on the Caraça ridge (east QF; Nunes 2016), Moeda syncline (west QF; Madeira *et al.* 2019) and Gandarela and Ouro Fino synclines (central-eastern QF; this study) (Tab. 5). According to these researches, the basal early syn-rift deposits of the Moeda Formation and, mainly, its upper paraconformity contact of transgressive surface with the Batatal Formation are the unique stratigraphic datum for regional correlations, unknown any existing guide layer with or without fossiliferous and/or volcanic content between them (as pointed out by Maxwell 1972).

According to the sedimentological features of the lithofacies associations herein interpreted, its stacking patterns, stratigraphic succession, thickness variations and spatial distribution, we proposed four tectono-sedimentary stages for the basin filling evolution of the rift basin in the Moeda Formation at Gandarela and Ouro Fino synclines (Fig. 10). Paleocurrent data were not obtained in this research; however, Lindsey (1975) attributed Westerly to Southwesterly as the paleoflow main direction in the Gandarela syncline, associated with the uplift of its source areas. According to Miall (2010), a

tectonic controlled sedimentary basin, as in the occurrence of the rift basin Moeda Formation, presents a paleocurrent direction perpendicular to its basin margin and towards the proximal-to-distal lithofacies association succession. In this sense, the NE-SW-trending basin margins and the succession of lithofacies association towards the Southeastern Gandarela and Ouro Fino synclines (Fig. 5) allowed us to infer a general Northwesterly to Southeasterly paleocurrent direction at the study area.

The first tectono-sedimentary stage is represented by an extensional tectonic regime, which was responsible for the development of normal faults in an early rift setting leading the opening of Gandarela and West Ouro Fino rift sub-basins (Fig. 10 and Tab. 5). The basement of both sub-basins were the Nova Lima Group (RVS) rocks, as identified by the U-Pb detrital zircon dating analysis of samples 1 and 1b in addition to the geologic mapping (Figs. 5 and 8). This tectono-sedimentary stage is materialized by the basal and syntectonic alluvial to fluvial fan deposits of the ALG1 and ALOF1 at the proximal zones of the normal fault edges. The normal faults highly controlled the sediment supply, the area distribution of the basal lithofacies associations and its main source areas. The main source areas for the ALG1 and ALOF1 were likely the adjacent horsts of the Nova Lima Group and uplifted Mesoarchean continental crusts, as suggested by the majority

Table 5. Regional correlation of the Moeda Formation stratigraphic succession from West (Moeda synclines) to East (Caraça range) of the Quadrilátero Ferrífero. In gray, the early syn-rift deposits can be seen as the regional basal datum. In pink, the paraconformity contact of transgressive surface as the regional top datum.

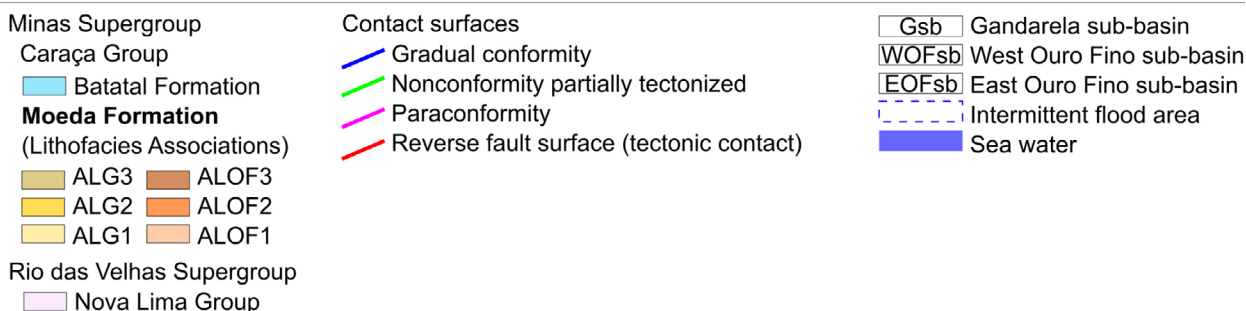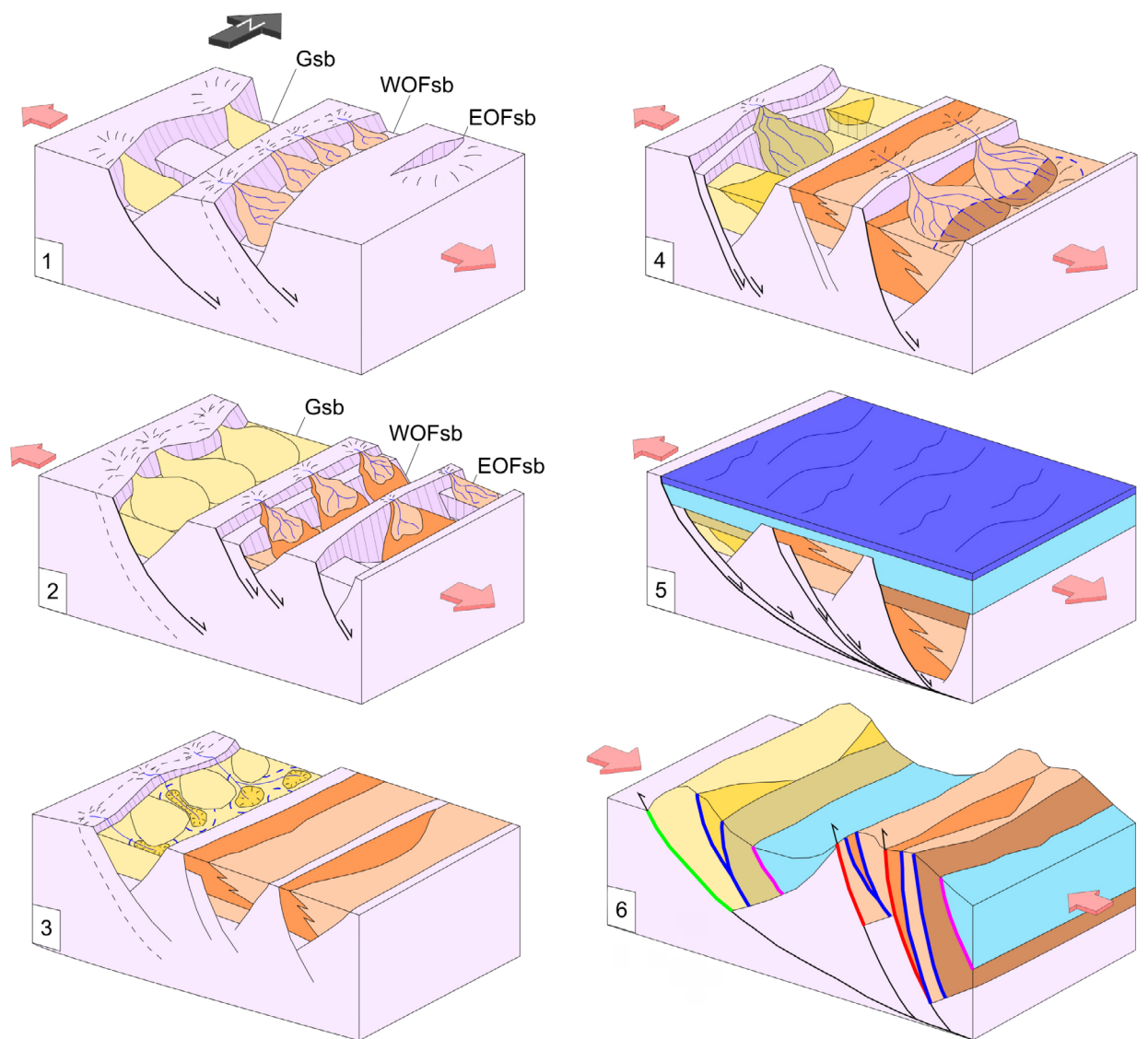| Formation	Tectonic setting	Tectono-sedimentary stage	Lithofacies associations			
			Moeda syncline (West QF) (Madeira *et al.* 2019)	Gandarela syncline (Central-eastern QF) (this study)	Ouro Fino syncline (Central-eastern QF) (this study)	Caraça range (East QF) (Nunes 2016)
Moeda	Early rift	(1st stage) First extensional tectonic activity	AF1 – Alluvial fan AF2 (base) – Braided rivers of a fluvial plain	ALG1 – Proximal zone of an alluvial fan	ALOF1 – Proximal zone of a fluvial fan system	Unit 1 – Proximal zone of an alluvial fan and braided rivers of an alluvial plain
	Rift	(2nd stage) Continuous opening and infilling	AF2 (top) AF3 – Lacustrine system associated with a shallow marine environment	-	ALOF2 – Alluvial fan dominated by debris flow	Unit 2 – Proximal zone of braided rivers and a fluvial fan with eolic reworking
		(3rd stage) Tectonic quiescence	-	ALG2 – Sheet flow of an alluvial floodplain	-	-
		(4th stage) Second extensional tectonic activity	AF4 (base) – Braided rivers of a fluvial plain	ALG3 – Fluvial fan system dominated by braided rivers with gravel bars	ALOF3 – Terminal fluvial fan	-
	Rift-to passive margin	-	AF4 (top) AF5 – Marine transgression	-	-	Unit 3 – Distal area of a braided rivers fluvial system with coastline formation
Paraconformity contact of transgressive surface						
Batatal	Passive margin	(5th stage) Extensional drift	Shallow marine metapelites			

Figure 10. Sketches displaying the tectono-sedimentary model for the basin filling evolution of Moeda Formation lithofacies association in the Southern Gandarela and Ouro Fino synclines as a Neoarchean/Paleoproterozoic rift basin.

of 2095-3185 Ma U-Pb detrital zircon ages obtained in the Moeda Formation (samples 4 and 6; Figs. 3 and 8).

On a sequence stratigraphy approach, the top gradual conformity surface limits of the ALG1 and ALOF1 can be categorized as key sequence stratigraphic surfaces (based on Catuneanu 2019 and Magalhães *et al.* 2020), due to marking changes in the Moeda Formation stacking patterns (from a fifth order coarsening-upward to a fifth order fining-upward cycle in the Gandarela syncline, and from a fifth order fining-upward to a fifth order coarsening-upward cycle at the

Ouro Fino syncline; Fig. 5). The sixth hierarchical order fining-upward cycles (oligomict conglomerates grading to massive sandstones) of ALG1 and ALOF1 indicate a high frequency lateral migration of its alluvial and fluvial channels (James and Dalrymple 2010, Catuneanu 2019), while the fifth hierarchical order coarsening and thickening upward cycles (sandstone predominance grading to massive conglomerate predominance) in the ALG1 indicate progradation of its alluvial fan deposits (Assine 2008, Miall 2016). According to the sequence stratigraphy of upstream-controlled settings (Catuneanu 2019),

the ALG1 fifth order stacking patterns can be interpreted as High-Amalgamation (channel-dominated) System Tracts. This interpretation was based on three main factors of ALG1:
- its coarsening and thickening in an upward cycle;
- its low rates of floodplain aggradation with no pelitic content;
- its high-frequency of alluvial channels lateral migration with high energy fluxes, which were influenced by the steep topographic gradient of their early-rift basin margins.

The second tectono-sedimentary basin evolution stage is represented by a continuity of extensional tectonic activity in a rift setting, leading a forced subsidence of the West and East Ouro Fino sub-basins and accommodation increasing (Fig. 10 and Tab. 5). This tectono-sedimentary stage is materialized by the rift related alluvial fan deposits of the ALOF2 in both sub-basins of Ouro Fino syncline. The high gravel content of the ALOF2 indicates an increase in flow energy and flow competency of its alluvial fan system, likely caused by two main factors (Catuneanu 2019):
- steepening of the topographic gradient of its rift sub-basin margins, as a result of the forced subsidence;
- the increase in discharge as a result of shifts to more humid climatic conditions.

The preserved metapelitic clasts on the ALOF2 clast-supported conglomerates lithofacies indicate at least one proximal source area, as these types of clasts commonly present a low mechanical resistance for long-distance sedimentary transports. The ALOF2 fifth order coarsening-upward cycle (increase in the clast diameter upward of the clast-supported conglomerates lithofacies) can indicate progradation events of alluvial fans (Assine 2008, Miall 2016). According to the sequence stratigraphy of upstream-controlled settings (Catuneanu 2019), the ALOF2 fifth order stacking patterns can be categorized as a High-Amalgamation (channel-dominated) System Tracts, as a result of its fifth order coarsening-upward cycle, its low rates of floodplain aggradation and high frequency of alluvial channel lateral migration.

The third tectono-sedimentary basin evolution stage is marked by reduced to absent tectonic activity in a rift quiescence setting (Fig. 10 and Tab. 5). The sedimentary filling in this stage is materialized by the ALG2 sheet flow deposits in the Gandarela sub-basin and by an overfilled accommodation in the Ouro Fino sub-basins. The predominance of fine- to medium-sized grains of the ALG2 indicates a reduction of both flow energy and competence (Miall 2010) compared to the previous tectono-sedimentary stages. Based on the presence of infiltrated clay, which is typical of an intermittent underwater deposition system (Boggs 2009), and the bottom limit of the ALG2 by a gradual conformity with the alluvial fans of ALG1, we interpret that the ALG2 sheet flow deposition occurred at a floodplain in the alluvial fans generated in the previous tectono-sedimentary stages. The sheet flow deposits of ALG2 show lenticular forms with no lateral continuity, which can be inferred as a result of deposition restricted to the topographic lows between the ALG1 alluvial fan lobes in distal portions (Fig. 10).

The fourth and last tectono-sedimentary stage herein inferred for the Moeda Formation rift basin evolution is represented by a new extensional tectonic period. This tectono-sedimentary stage resulted in the subsidence of the Southern Gandarela and West Ouro Fino sub-basins by the reactivation of preexisting normal faults in a rift setting, while the East Ouro Fino overfilled sub-basin worked as a structural high (horst) (Fig. 10 and Tab. 5). The sedimentary filling in this stage is materialized by the ALG3 fluvial fan deposits in the Gandarela sub-basin and the ALOF3 terminal fluvial fan deposits in the East Ouro Fino sub-basin. Based on Assine (2008) and Miall (2010, 2016), the ALG3 sixth order fining-upward sedimentary cycles (massive oligomict conglomerates grading to sandstones) indicate an intense fluvial channel lateral migration, while its fifth order fining-upward sedimentary cycles (conglomerate predominance grading to sandstone predominance) indicate a general stacking pattern of decelerating fluxes with competence reduction. The presence of infiltrated clay minerals on ALOF3 is indicative of an intermittent underwater sedimentary environment (Boggs 2009) at distal flood zones of the previous fluvial fans (Fig. 10).

Based on our stratigraphic and structural data, we could propose two additional tectono-sedimentary stages of posterior Moeda Formation deposition:
- the fifth stage, which is represented by the formation of a passive margin in an extensional drift tectonic setting;
- the sixth stage, which is represented by tectonic inversion (Fig. 10).

At the fifth tectono-sedimentary stage, the Moeda Formation lithofacies associations were completely covered by the shallow marine deposits of the Batatal Formation, as a result of a transgressive event related to passive margin formation and generalized subsidence of the entire previous rift sub-basins (Fig. 10). This stratigraphic succession marks the Moeda Formation's upper limit as a paraconformity contact of transgressive surface, one of the best data for the Moeda Formation's regional correlations (Tab. 5).

The sixth tectono-sedimentary stage was responsible for the reactivation of preexisting normal to thrust-reverse faults in a compressional setting, explaining the current stratigraphic inversion of the basal (Nova Lima Group) and top (Batatal Formation) bounds of the Moeda Formation in the study area (Fig. 10).

CONCLUSION

The Moeda Formation (base of Caraça Group, MS), in the Southernmost Gandarela and Ouro Fino synclines (Central-Eastern portion of the QF), reveals sedimentary characteristics of an intracontinental rift basin evolution, representing the first tectono-sedimentary rift stages of the Minas Basin. According to sedimentological, stratigraphic and U-Pb detrital zircon dating analysis presented, it is possible to conclude:
- the stratigraphic sequence of the Moeda Formation can be subdivided into three lithofacies associations in the Gandarela syncline (ALG1, ALG2, ALG3) and three

others in the Ouro Fino syncline (ALOF1, ALOF2 and ALOF3). The ALG1, ALOF1 and ALOF2 represent proximal alluvial and fluvial fan deposits with a predominance of oligomict clast-supported conglomerates as the basal depositional sequences. The ALG2 is the upper lithofacies association that is related to sheet flow in an alluvial floodplain deposition system, mainly constituted by quartz-arenite beds. Finally, the ALG3 and ALOF3 represent the top sequences, which are related to distal zones in fluvial fan deposits, mainly constituted by massive sandstones;

- the detrital zircon ^{207}Pb/^{206}Pb ages of the Moeda Formation show a youngest cluster at 2777 ± 14 Ma, with the following main source areas: late Mesoarchean continental crust, Meso-to Neoarchean RVS, and Archean TTG complexes;

- detrital zircon ^{207}Pb/^{206}Pb ages of the Nova Lima Group (RVS) and the Batatal Formation (top of Caraça Group, MS) show completely different spectra, with the youngest clusters falling into the ages of 2716 ± 10 Ma and 2786 ± 9 Ma, respectively. These results contributed in identifying stratigraphic inversions at the bottom and upper normal limits of the Moeda Formation and indicating the Nova Lima Group as the basement of the Moeda rift basin in the study area;

- based on our data and literature correlations, the deposition age of the Moeda Formation must be between 2716 Ma (Nova Lima Group youngest cluster detrital zircon age herein obtained) and 2520 Ma (youngest Moeda Formation depositional age dated by Nunes 2016);

- the chronostratigraphic inversion of the Moeda Formation (2777 ± 14 Ma) and Nova Lima Group's (2716 ± 10 Ma) youngest clusters of detrital zircon ages indicate a progressive exhumation of the common source areas (Archean TTG complexes) or a contribution from younger K-rich granitoids of the Mamona I event to the Nova Lima Group;

- the upper limit of the Moeda Formation, represented by a paraconformity contact of transgressive surface with the overlapped Batatal Formation, is one of the best data for the Moeda Formation's regional correlations.

REFERENCES

Aguilar C., Alkmim F.F., Lana C., Farina F. 2017. Palaeoproterozoic assembly of the São Francisco craton, SE Brazil: New insights from U–Pb titanite and monazite dating. *Precambrian Research*, **289**:95-115. https://doi.org/10.1016/j.precamres.2016.12.001

Alkmim F.F., Lana C. de C., Duque T.R.F. 2014. Zircões detríticos do Grupo Itacolomi e o registro do soerguimento do Cinturão Mineiro. *In*: Congresso Brasileiro de Geologia, 47., Salvador. *Anais*, p. 1802.

Alkmim F.F., Marshak S. 1998. Transamazonian Orogeny in the Southern São Francisco Craton Region, Minas Gerais, Brazil: evidence for Paleoproterozoic collision and collapse in the Quadrilátero Ferrífero. *Precambrian Research*, **90**(1-2):29-58. https://doi.org/10.1016/S0301-9268(98)00032-1

Alkmim F.F., Martins-Neto M.A. 2012. Proterozoic first-order sedimentary sequences of the São Francisco craton, eastern Brasil. *Marine and Petroleum Geology*, **33**(1):127-139. https://doi.org/10.1016/j.marpetgeo.2011.08.011

Alkmim F.F., Teixeira W. 2017. The Paleoproterozoic Mineiro Belt and the Quadrilátero Ferrífero. *In*: Heilbron M., Cordani U.G., Alkmim F.F. (Eds.). *São Francisco Craton, eastern Brazil:* tectonic genealogy of a miniature continent. New York: Springer Berlin Heidelberg, p. 71-94.

Almeida F.F.M. 1977. O cráton do São Francisco. *Revista Brasileira de Geociências*, **7**:349-364.

Assine M.L. 2008. Ambientes de Leques Aluviais. In: Pedreira da Silva A.J.C.L., Aragão M.A.N.F., Magalhães A.J.C. (Eds.). *Ambientes de sedimentação siliciclástica do Brasil*. São Paulo: Beca, p. 52-70.

Baltazar O.F., Baars F.J., Lobato L.M., Reis L.B., Achtschin A.B., Berni G.V., Silveira V.D. 2005. Mapa Geológico Gandarela na Escala 1:50.000. Nota Explicativa. In: Lobato L.M., Baltazar O.F., Reis L.B., Achtschin A.B., Baars F.J., Timbó M.A., Berni G.V., de Mendonça B.R.V., Ferreira D.V. (Eds.). *Projeto Geologia do Quadrilátero Ferrífero Integração e Correção Cartográfica em SIG com Nota Explicativa*. Belo Horizonte: CODEMIG, 68 p.

Baltazar O.F., Zucchetti M. 2007. Lithofacies associations and structural evolution of the Archean Rio das Velhas greenstone belt, Quadrilátero Ferrífero, Brazil: A review of the setting of gold deposits. *Ore geology Reviews*, **32**(3-4):471-499. https://doi.org/10.1016/j.oregeorev.2005.03.021

Boggs S. 2009. *Petrology of sedimentary rocks*. New York: Cambridge University, 600 p.

Campos J.C.S., Carneiro M.A., Basei M.A.S. 2003. U-Pb evidence for Late Neoarchean crustal reworking in the Southern São Francisco Craton (Minas Gerais, Brazil). *Anais da Academia Brasileira de Ciências*, **75**(4):497-511. https://doi.org/10.1590/S0001-37652003000400008

Cassino L.F. 2014. *Distribuição de idades de zircões detríticos dos supergrupos Rio das Velhas e Minas na Serra de Ouro Preto, Quadrilátero Ferrífero, MG - implicações para a evolução sedimentar e tectônica*. Monography, Departamento de Geologia, Universidade Federal de Ouro Preto, Ouro Preto, 53 p.

Catuneanu O. 2019. Model-independent sequence stratigraphy. *Earth-Science Reviews*, **188**:312-388. https://doi.org/10.1016/j.earscirev.2018.09.017

Cederberg J., Söderlund U., Oliveira E., Ernst R., Pisarevsky S. 2016. U-Pb baddeleyite dating of the Proterozoic Pará de Minas dyke swarm in the São Francisco craton (Brazil) – implications for tectonic correlation with Siberia, Congo and the North China cratons. *GFF*, **138**(1):219-240. https://doi.org/10.1080/11035897.2015.1093543

Chemale Jr. F., Rosière C.A., Endo I. 1994. The tectonic evolution of the Quadrilátero Ferrífero, Minas Gerais, Brazil. *Precambrian Research*, **65**(1-4):25-54. https://doi.org/10.1016/0301-9268(94)90098-1

Condie K.C. 2014. Growth of continental crust: a balance between preservation and recycling. *Mineralogical Magazine*, **78**(3):623-637. https://doi.org/10.1180/minmag.2014.078.3.11

Corfu F., Hanchar J.M., Hoskin P.W.O., Kinny P. 2003. Atlas of Zircon Textures: Reviews in Mineralogy and Geochemistry, **53**(1):469-500. https://doi.org/10.2113/0530469

Dickinson W.R., Gehrels G.E. 2009. Use of U-Pb ages of detrital zircons to infer maximum depositional ages of strata: A test against a Colorado Plateau Mesozoic database. *Earth and Planetary Science Letters*, **288**(1-2):115-125. https://doi.org/10.1016/j.epsl.2009.09.013

Dopico C.I.M., Lana C., Moreira H.S., Cassino L.F., Alkmim F.F. 2017. U-Pb ages and Hf-isotope data of detrital zircons from the late Neoarchean-Paleoproterozoic Minas Basin, SE Brazil. *Precambrian Research*, **291**:143-161. https://doi.org/10.1016/j.precamres.2017.01.026

Dorr II J.V.N. 1969. Physiographic, Stratigraphic and Structural Development of the Quadrilátero Ferrífero, Minas Gerais, Brazil. Washington: USGS/DNPM Geological Survey Professional Paper, 117 p. https://doi.org/10.3133/pp641A

Duque T., Alkmim F., Lana, C. 2020. Grãos detríticos de zircão do Grupo Itacolomi em sua área tipo, Quadrilátero Ferrífero, Minas Gerais: idades, proveniência e significado tectônico. *Geologia USP. Série Científica*, **20**(1):101-123. https://doi.org/10.11606/issn.2316-9095.v20-151397

Dutra L.F., Dias S.P., Martins M., Lana C., Batista A.C., Tavares, T.D. 2020. Detrital zircon records of the Paleo-Mesoproterozoic rift-sag Tamanduá Group in its type-section, Northern Quadrilátero Ferrífero, Minas Gerais, Brazil. *Brazilian Journal of Geology*, **50**(1):e20190069. https://doi.org/10.1590/2317-4889202020190069

Dutra L.F., Martins M., Lana C. 2019. Sedimentary and U-Pb detrital zircons provenance of the Paleoproterozoic Piracicaba and Sabará groups, Quadrilátero Ferrífero, Southern São Francisco craton, Brazil. *Brazilian Journal of Geology*, **49**(2):1-21. https://doi.org/10.1590/2317-4889201920180095

Einsele G. 2000. *Sedimentary basins:* evolution, facies, and sediment budget. Berlin: Springer Verlag, 628 p.

Endo I., Fonseca M.A. 1992. Sistema de cisalhamento Fundão-Cambotas no Quadrilátero Ferrífero, geometria e cinemática. *Revista Escola de Minas*, **45**(1-2):15-17.

Endo I., Machado R. 2002. Reavaliação e novos dados geocronológicos (Pb/Pb e K/Ar) da região do Quadrilátero Ferrífero e adjacências. *Geologia USP. Série Científica*, **2**:23-40. https://doi.org/10.5327/S1519-874X2002000100005

Farina F., Albert C., Lana C. 2015. The Neoarchean transition between medium and high K granitoids: Clues from the Southern São Francisco Craton (Brazil). *Journal of South American Earth Sciences*, **266**:375-394. https://doi.org/10.1016/j.precamres.2015.05.038

Farina F., Albert C., Martínez Dopico C., Aguilar Gil C., Moreira H., Hippertt J., Cutts K., Alkmim F., Lana C. 2016. The Archean-Paleoproterozoic evolution of the Quadrilátero Ferrífero (Brasil): current models and open questions. *Journal of South America Earth Sciences*, **68**:4-21. https://doi.org/10.1016/j.jsames.2015.10.015

Grant M.L, Wilde S.A., Wu F., Yang J. 2009. The application of zircon cathodoluminescence imaging, Th-U-Pb chemistry and U-Pb ages in interpreting discrete magmatic and high-grade metamorphic events in the North China Craton at the Archean/Proterozoic boundary: *Chemical Geology*, **261**(1-2):155-171. https://doi.org/10.1016/j.chemgeo.2008.11.002

Harley S.L., Kelly N.M., Möller A. 2007. Zircon Behaviour and the Thermal Histories of Mountain Chains. *Elements*, **3**(1):25-30. https://doi.org/10.2113/gselements.3.1.25

Hartmann A., Endo I., Suita M.T.F., Santos J.O.S., Frantz J.C., Carneiro M.A., McNaughton N.J., Barley M.E. 2006. Provenance and age delimitation of Quadrilátero Ferrífero sandstones based on zircon U–Pb isotopes. *Journal of South American Earth Sciences*, **20**(4):273-285. https://doi.org/10.1016/j.jsames.2005.07.015

Hartmann L.A., Leite J.A.D., Da Silva L.C., Remus M.V.D., McNaughton N.J., Groves D.I., Fletcher I.R., Santos J.O.S., Vasconcellos M.A.Z. 2000. Advances in SHRIMP geochronology and their impact on understanding the tectonic and metallogenic evolution of southern Brazil. *Australian Journal of Earth Sciences*, **47**(5):829-844. https://doi.org/10.1046/j.1440-0952.2000.00815.x

Hoskin P.W.O., Black L.P. 2000. Metamorphic zircon formation by solid-state recrystallization of protolith igneous zircon. *Journal of Metamorphic Geology*, **18**(4):423-439. https://doi.org/10.1046/j.1525-1314.2000.00266.x

Jackson S.E., Pearson N.J., Griffin W.L., Belousova E.A. 2004. The application of laser ablation-inductively coupled plasma-mass spectrometry to in situ U-Pb zircon geochronology. *Chemical Geology*, **211**(1-2):47-69. https://doi.org/10.1016/j.chemgeo.2004.06.017

James N.P., Dalrymple R.W. 2010. *Facies Models*. 4th ed. Canada: Geological Association of Canada, 586 p.

Koglin N., Zeh A., Cabral A.R., Gomes Jr. A.A.S., Corrêa Neto A.V., Brunetto W.J., Galbiatti H. 2014. Depositional age and sediment source of the auriferous Moeda Formation, Quadrilátero Ferrífero of Minas Gerais, Brazil: New constraints from U–Pb–Hf isotopes in zircon and xenotime. *Precambrian Research*, **255**(Part 1):96-108. https://doi.org/10.1016/j.precamres.2014.09.010

Lana C., Alkmim F.F., Armstrong R., Scholz R., Romano R., Nalini Jr. H.A. 2013. The ancestry and magmatic evolution of Archaean TTG rocks of the Quadrilátero Ferrífero province, southeast Brazil. *Precambrian Research*, **231**:157-173. https://doi.org/10.1016/j.precamres.2013.03.008

Lewis M.M., Jackson C.A.L., Gawthorpe R.L. 2015. Tectono-sedimentary development of early syn-rift deposits: the Abura Graben, Suez Rift, Egypt. *Basin Research*, **29**(S1):327-351. https://doi.org/10.1111/bre.12151

Lindsey D.A. 1975. *Depositional environments and paleocurrent directions in the Precambrian Moeda Formation, Minas Gerais, Brazil*. U.S. Geology Survey, 22 p.

López-Sanchéz M.A., Aleinikoff J.N., Marcos Vallaure A., Martínez F.J., Llana-Fúnez S. 2016. An example of low-Th/U zircon overgrowths of magmatic origin in a late orocegenic Variscan intrusion: the San Ciprián massif (NW Spain). *Journal of the Geological Society*, **173**(2):282-291. http://dx.doi.org/10.1144/jgs2015-071

Ludwig K.R. 2012. *User's Manual for Isoplot 3.75*. Berkeley: Berkeley Geochronology Center No. 5, 75 p.

Machado N., Schrank A., Noce C.M., Gauthier G. 1996. Ages of detrital zircon from Archean-Paleoproterozoic sequences: Implications for Greenstone Belt setting and evolution of a Transamazonian foreland basin in Quadrilátero Ferrífero, southeast Brazil. *Earth and Planetary Science Letters*, **141**(1-4):259-276. https://doi.org/10.1016/0012-821X(96)00054-4

Madeira M.R., Martins M.S., Martins G.P., Alkmim F.F. 2019. Caracterização faciológica e evolução sedimentar da Formação Moeda (Supergrupo Minas) na porção noroeste do Quadrilátero Ferrífero, Minas Gerais. *Geologia USP. Série Científica*, **19**(3):129-148. http://dx.doi.org/10.11606/issn.2316-9095.v19-148467

Madureira R.S. 2020. *Caracterização faciológica da Formaçao Moeda (Grupo Caraça, Supergrupo Minas) e estudos geocronológicos U-Pb nos sinclinais Gandarela e Ouro Fino, Quadrilátero Ferrífero, Minas Gerais.* MS Dissertation, Departamento de Geologia, Universidade Federal de Ouro Preto, Ouro Preto, 98 p.

Magalhães A.J.C., Raja Gabaglia G.P., Fragoso D.G.C., Bento Freire E., Lykawaka R., Arregui C.D., Silveira M.M.K., Carpio K.M.T., De Gasperi A., Pedrinha S., Artagão V.M., Terra G.J.S., Bunevich R.B., Roemers-Oliveira E., Gomes J.P., Hernández J.I., Hernández R.M., Bruhn C.H.L. 2020. High-resolution sequence stratigraphy applied to reservoir zonation and characterisation, and its impact on production performance – shallow marine, fluvial downtream, and lacustrine carbonate settings. *Earth-Science Reviews*, **210**:103325. https://doi.org/10.1016/j.earscirev.2020.103325

Maxwell C.H. 1972. *Geology and ore deposits of the Alegria district, Brazil.* Washington: USGS/DNPM, Professional Paper 341-J, 72 p.

Miall A.D. 1996. *The Geology of Fluvial Deposits:* Sedimentary Facies, Basin Analysis and Petroleum Geology. Berlin: Springer-Verlag, 582 p.

Miall A.D. 2000. *Principles of sedimentary basin analysis.* 3rd ed. Canada: Springer-Verlag Berlin Heidelberg, 616 p.

Miall A.D. 2010. *The geology of stratigraphic sequences.* Berlin: Springer-Verlag, 522 p.

Miall A.D. 2016. *Stratigraphy:* A Modern Synthesis. Toronto: Springer, 454 p.

Minter W.E.L., Renger F.E., Sierges A. 1990. Early Proterozoic gold placers of the Moeda Formation within the Gandarela Syncline, Minas Gerais, Brazil. *Bulletin of the Society of Economic Geologists*, **85**(5):943-951. https://doi.org/10.2113/gsecongeo.85.5.943

Moraes M.A.S. 1985. Reconhecimento de fácies sedimentares em rochas metamórficas da região de Ouro Preto (MG). *In*: Simpósio de Geologia de Minas Gerais, 3., 1985. *Anais...*, **5**:84-90.

Moreira H.S., Lana C., Nalini Jr H.A. 2016. The detrital zircon record of an Archaean convergent basin in the Southern São Francisco Craton, Brazil. *Precambrian Research*, **275**:84-99. https://doi.org/10.1016/j.precamres.2015.12.015

Noce C., Zuccheti M., Baltazar O., Armstrong R., Dantas E., Renger F., Lobato L. 2005. Age of felsic volcanism and the role of ancient continental crust in the evolution of the Neoarchean Rio das Velhas Greenstone Belt (Quadrilátero Ferrífero, Brazil): U-Pb zircon dating of volcaniclastic graywackes. *Precambrian Research*, **141**(1-2):67-82. https://doi.org/10.1016/j.precamres.2005.08.002

Nunes F.S. 2016. *Contribuição à estratigrafia e geocronologia U-Pb de zircões detríticos da Formação Moeda (Grupo caraça, Supergrupo Minas) na Serra do Caraça, Quadrilátero Ferrífero, Minas Gerais.* Ms Dissertation. Departamento de Geologia, Universidade Federal de Ouro Preto, Ouro Preto, 77 p.

Queiroz Y.S., Queiroga G., Moraes R., Fernandes V.M.T., Medeiros-Júnior E., Jordt-Evangelista H., Schulz B., Schmiedel J., Martins M., Castro M.P., Lana C. 2019. Pseudosection modeling and U-Pb geochronology on Piranga schists: role of Brasiliano Orogeny in the Southeastern Quadrilátero Ferrífero, Minas Gerais, Brazil. *Brazilian Journal of Geology*, **49**(3):1-19. http://dx.doi.org/10.1590/2317-4889201920180136

Reading H.G. 1986. *Sedimentary Environments:* Processes, Facies and Stratigraphy. Massachusetts: Blackwell, 704 p.

Reading H.G. 1996. *Sedimentary Environments:* Processes, Facies and Stratigraphy. Massachusetts: Blackwell, 688 p.

Renger F.E., Noce C.M., Romano A.W., Machado N. 1994. Evolução sedimentar do Supergrupo Minas: 500 Ma de registro geológico no Quadrilátero Ferrífero, Minas Gerais, Brasil. *Genomos*, **2**(1):1-11. https://doi.org/10.18285/geonomos.v2i1.227

Romano R., Lana C., Alkmim F.F., Stevens G., Armstrong R. 2013. Stabilization of the southern portion of the São Francisco craton, SE Brazil, through a long-lived period of potassic magmatism. *Precambrian Research*, **224**:143-159. https://doi.org/10.1016/j.precamres.2012.09.002

Rosseto J.A., Alkmin F.F., Pereira M.M. 1987. Litofácies e modelo deposicional para a Formação Cambotas no maciço do Caraça. *In*: Simpósio de Sistemas Deposicionais do Pré-Cambriano, 1., 1987. *Roteiro de excursões*.

Rossignol C., Lana C., Alkmim F. 2020. Geodynamic evolution of the Minas Basin, southern São Francisco Craton (Brazil), during the early Paleoproterozoic: Climate or tectonic? *South American Earth Sciences*, **101**:102628. https://doi.org/10.1016/j.jsames.2020.102628

Rubatto D. 2017. Zircon: The Metamorphic Mineral. *Reviews in Mineralogy and Geochemistry*, **83**(1):261-295. https://doi.org/10.2138/rmg.2017.83.9

Santos M.M., Lana C., Scholz R., Buick I., Schmitz M.D., Kamo S.L., Gerdes A., Corfu F., Tapster S., Lancaster P., Storey C.D., Basei M.A.S., Tohver E., Alkmim A.R., Nalini H., Krambrock K., Fantini C., Wiedenbeck M. 2017. A New Appraisal of Sri Lankan BB Zircon as a Reference Material for LA-ICP-MS U-Pb Geochronology and Lu-Hf Isotope Tracing. *Geostandards and Geoanalytical Research*, **41**(3):335-358. https://doi.org/10.1111/ggr.12167

Sharman G.R., Malkowski M.A. 2020. Needles in a haystack: Detrital zircon U Pb ages and the maximum depositional age of modern global sediment. *Earth-Science Reviews*, **203**:103109. http://doi.org/10.1016/j.earscirev.2020.103109

Silva A.M., Chemale Jr. F., Kumuyumjian R.M., Heaman L. 1995. Mafic dike swarms of Quadrilátero Ferrífero and Southern Espinhaço, Minas Gerais, Brazil. *Revista Brasileira de Geociências*, **25**(**2**):124-137.

Sláma J., Košler J., Condon D.J., Crowley J.L., Gerdes A., Hanchar J.M., Horstwood M.S.A., Morris G.A., Nasdala L., Norberg N., Schaltegger U., Schoene B., Tubrett M.N., Whitehouse M.J. 2008. Plešovice zircon – a new natural reference material for U-Pb and Hf isotopic microanalysis. *Chemical Geology*, **249**(1-2):1-35. https://doi.org/10.1016/j.chemgeo.2007.11.005

Stow D.A.V. 2005. *Sedimentary Rocks in the Field:* A Colour Guide. London: Manson, 320 p.

Teixeira W., Ávila C.A., Dussin I.A., Corrêa Neto A.V., Bongiolo E.M., Santos J.O., Barbosa N.S. 2015. A juvenile accretion episode (2,35-2,32 Ga) in the Mineiro belt and its role to the Minas accretionary orogeny: zircon U-Pb-Hf and geochemical evidences. *Precambrian Research*, **256**:148-169. https://doi.org/10.1016/j.precamres.2014.11.009

Tucker M.E. 2001. *Sedimentary petrology:* An Introduction to the Origin of Sedimentary Rocks. Oxford: Blackwell Science, 262 p.

van Achterbergh E., Ryan C.G., Jackson S.E., Griffin W. 2001. Data Reduction software for LA-ICP-MS. *In*: Sylvester P. (Ed.). *Laser Ablation ICPMS in the Earh Science*. Canada: Mineralogical Association of Canada, p. 239-243.

Vavra G., Schmid R., Gebauer D. 1999. Internal morphology, habit and U-Th-Pb microanalysis of amphibolite-to-granulite facies zircons: geochronology of the Ivrea Zone (Southern Alps): *Contributions to Mineralogy and Petrology*, **134**:380-404. https://doi.org/10.1007/s004100050492

Villaça J.N. 1981. Alguns aspectos sedimentares da Formação Moeda. *Boletim da Sociedade Brasileira de Geologia Núcleo Minas Gerais*, **2**:93-137.

Villaça J.N., Moura L.A.M. 1981. Uranium in Precambrian Moeda Formation, Minas Gerais, Brazil. *In*: USGS (Ed.). *USGS Professional Paper A-BB Genesis of uranium and gold-bearing Precambrian quartz-pebble conglomerates*, United States, p. 1-14.

Walker R.G. 1992. Facies, facies models and modern stratigraphic concepts. *In*: Walker R.G., James N.P. *Facies Models:* Response to Sea Level. Canada: Geological Association of Canada, p. 1-14.

Wallace R.M. 1958. The Moeda Formation. *Boletim da Sociedade Brasileira de Geologia*, **7**(2):59-60.

Whitney D.L., Evans B.W. 2010. Abbreviations for names of rock-forming minerals. *American Mineralogist*, **95**(1):185-187. https://doi.org/10.2138/am.2010.3371

Zuccchetti M., Baltazar O.F., Raposo F.O. 1998. Estratigrafia. *In*: Pinto C.P. (Coord.). *Projeto Rio da Velhas Mapa Geológico Integrado.* Escala 1:100.000. Texto explicativo. Belo Horizonte: CPRM, p. 13-42.